Electronic Supplementary Information for

Cytotoxic evaluation and DNA interaction of Ru^{II}-bipy complexes containing coumarin-based ligands

Patrícia S. V. B. de Almeida[a], Henrique Jefferson de Arruda[a], Gleyton Leonel S. Sousa[a], Felipe Vitório Ribeiro[a], José Aleixo de Azevedo-França[b], Larissa A. Ferreira[a], Guilherme P. Guedes[c], Heveline Silva[d], Arthur E. Kummerle[a] and Amanda P. Neves[a]*

[a]Instituto de Química, Universidade Federal Rural do Rio de Janeiro, BR 465 Km 7, 23890-000, Seropédica, RJ, Brazil. E-mail: amandanevess@ufrrj.br

[b]Instituto de Ciências Exatas, Departamento de Química, Universidade Federal de Juiz de Fora, MG, Brazil.

[c]Instituto de Química, Universidade Federal Fluminense, Niterói, RJ, Brazil.

[d]Instituto de Ciências Exatas, Departamento de Química, Universidade Federal de Minas Gerais, MG, Brazil.

SUMMARY

I. Ethyl 3-(6-methyl-2-oxo-2*H*-chromen-3-yl)-3-oxopropanoate **(HL1)**

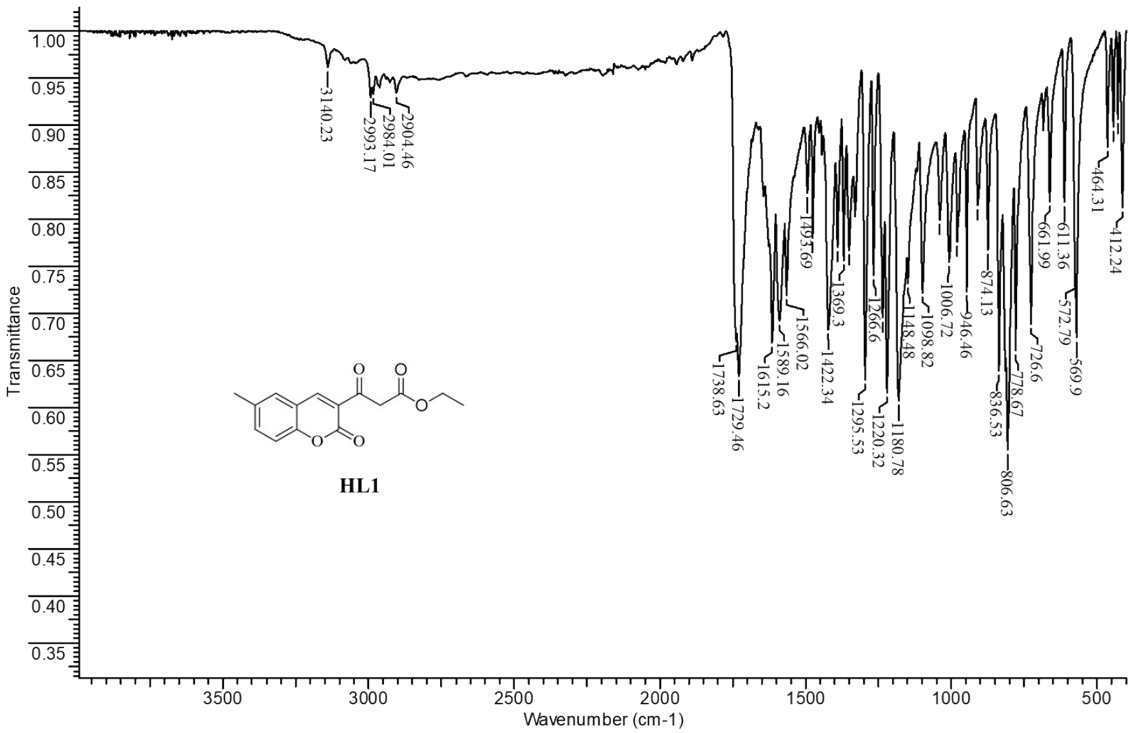

Figure S1: IR spectrum of **HL1**.

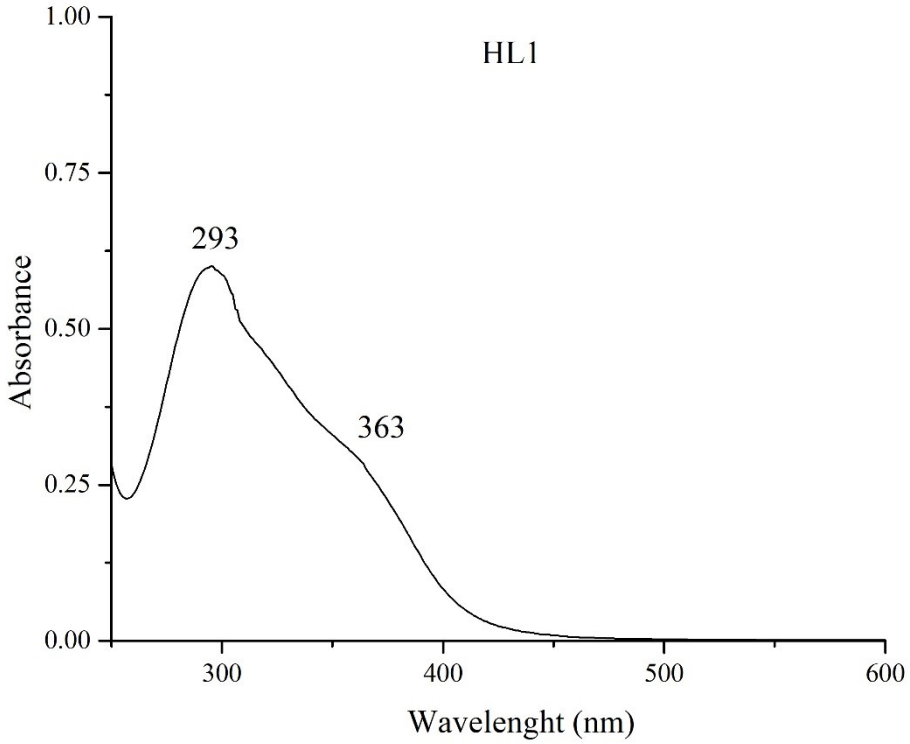

Figure S2: UV-Vis spectrum of **HL1** in phosphate buffer at 5 x 10^{-5} M.

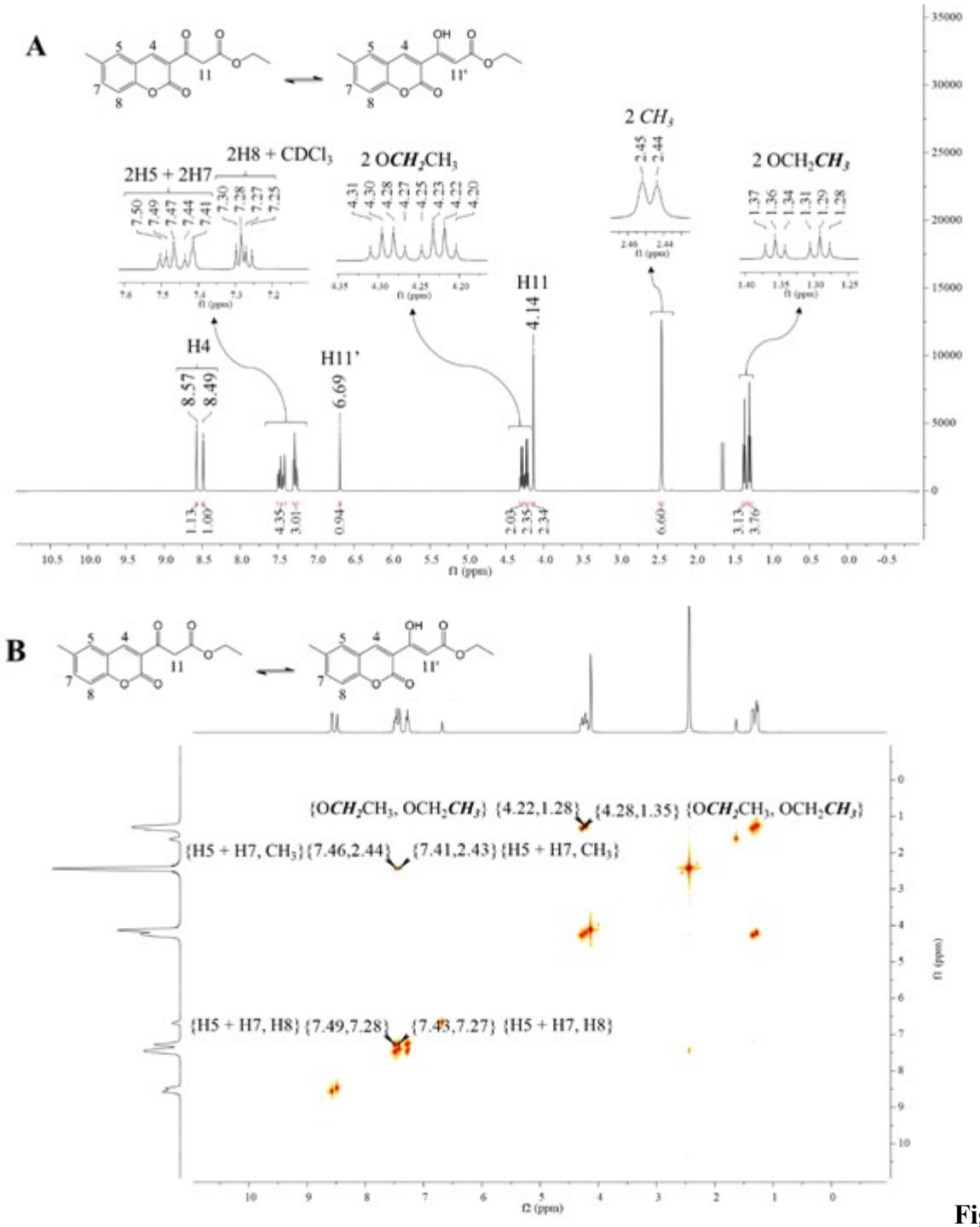

Figure S3: ^{1}H NMR spectrum of **HL1 (A)** and COSY spectrum **(B)**. Solvent: $CDCl_3$.

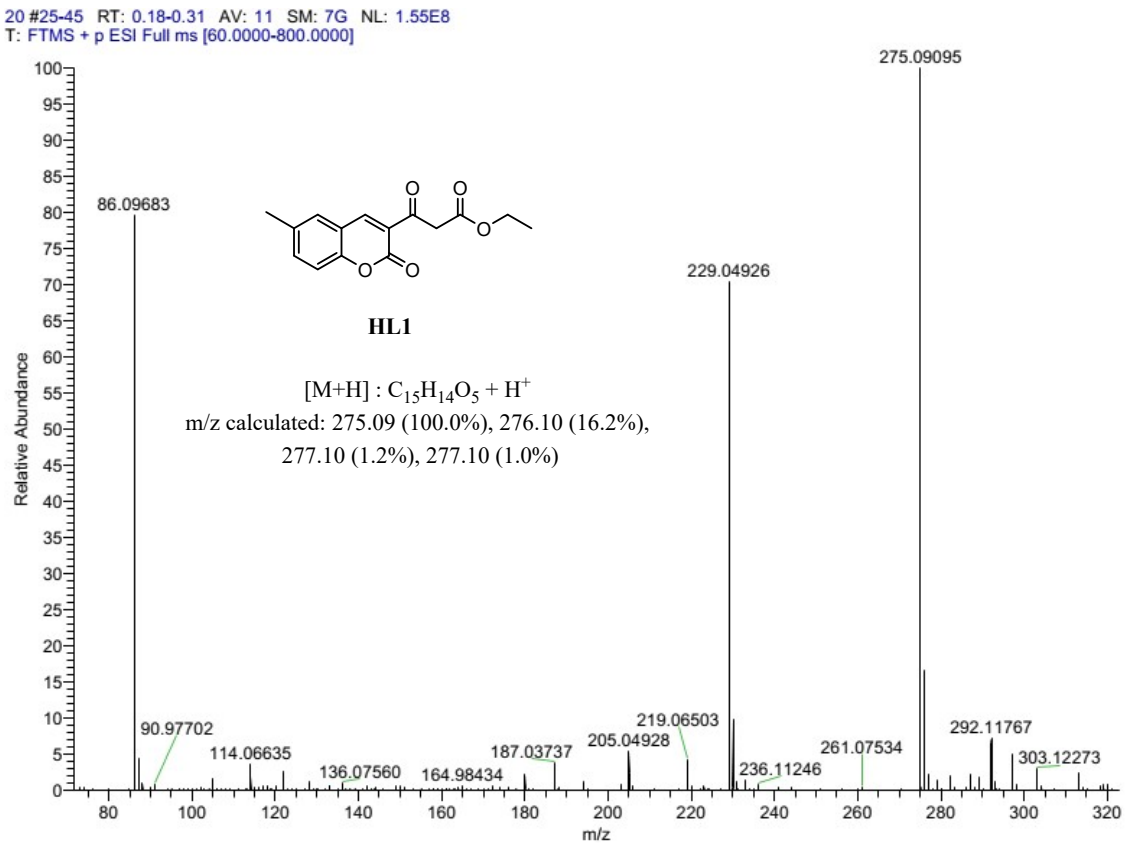

Figure S4: MS/ESI mass spectrum of **HL1**.

II. Ethyl 3-(7-(diethylamino)-2-oxo-2*H*-chromen-3-yl)-3-oxopropanoate **(HL2)**

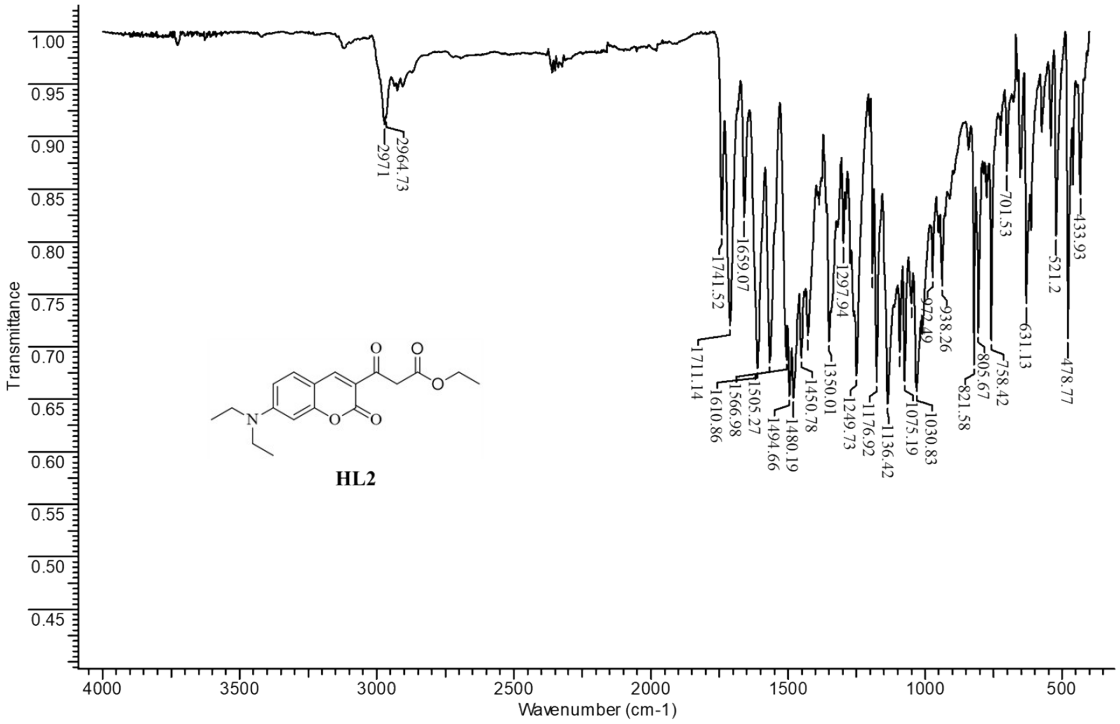

Figure S5: IR spectrum of **HL2**.

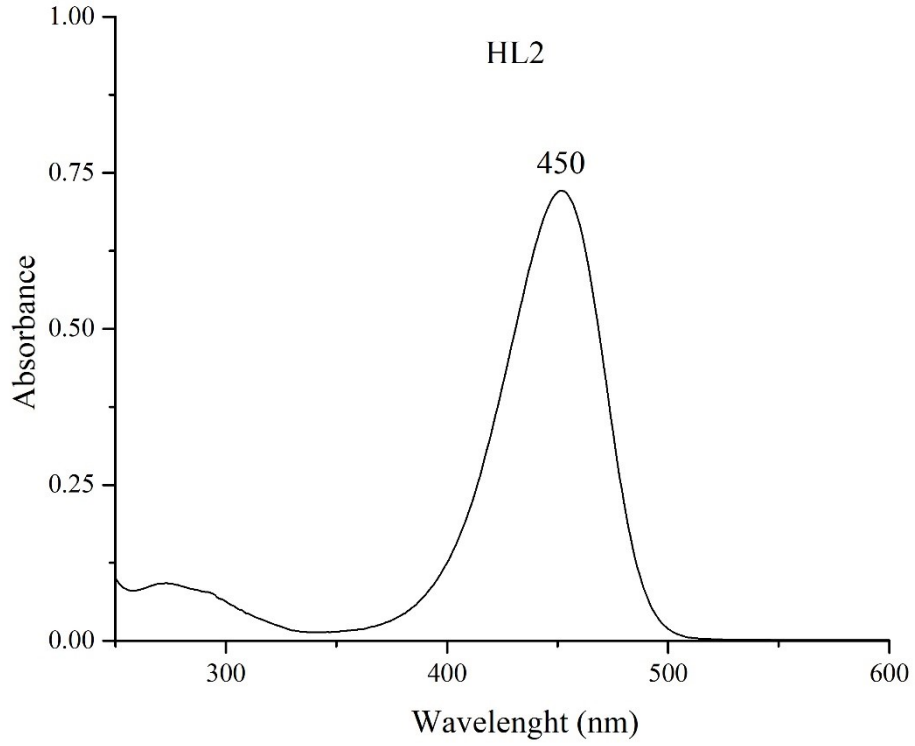

Figure S6: UV-Vis spectrum of **HL2** in phosphate buffer at 2 x 10^{-5} M.

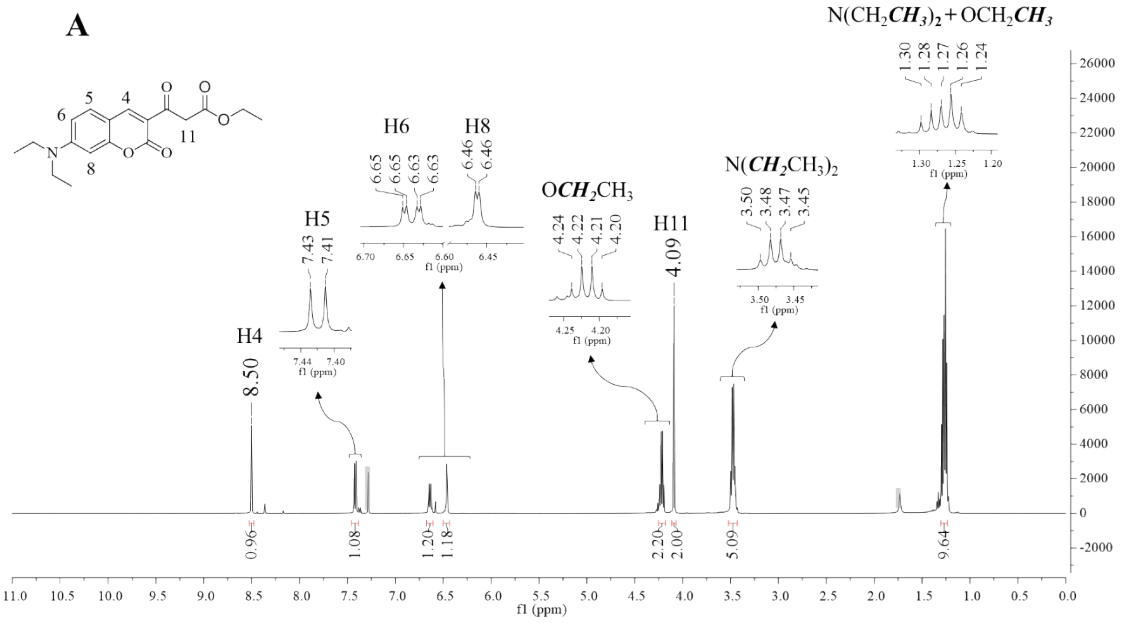

Figure S7: ^{1}H NMR spectrum of **HL2 (A)**. Solvent: $CDCl_3$.

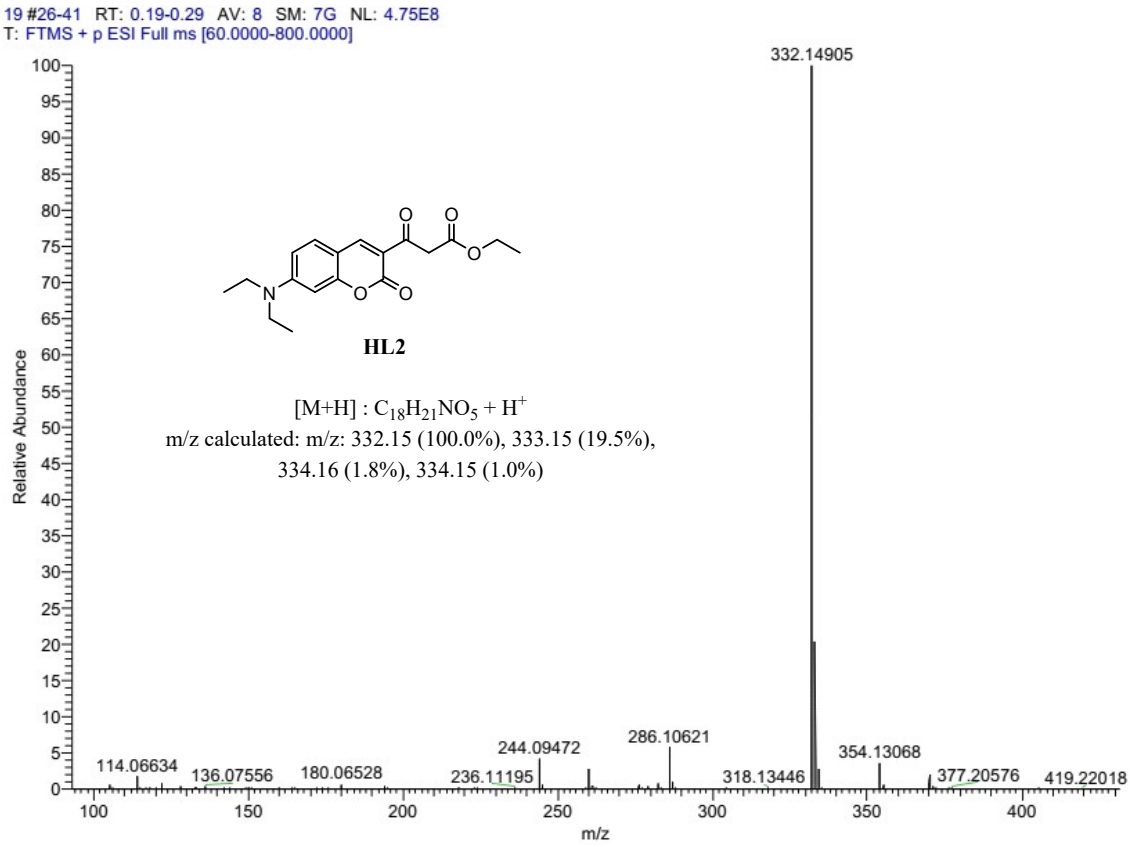

Figure S8: MS/ESI mass spectrum of **HL2**.

III. Ethyl 3-(8-methoxy-2-oxo-2*H*-chromen-3-yl)-3-oxopropanoate **(HL3)**

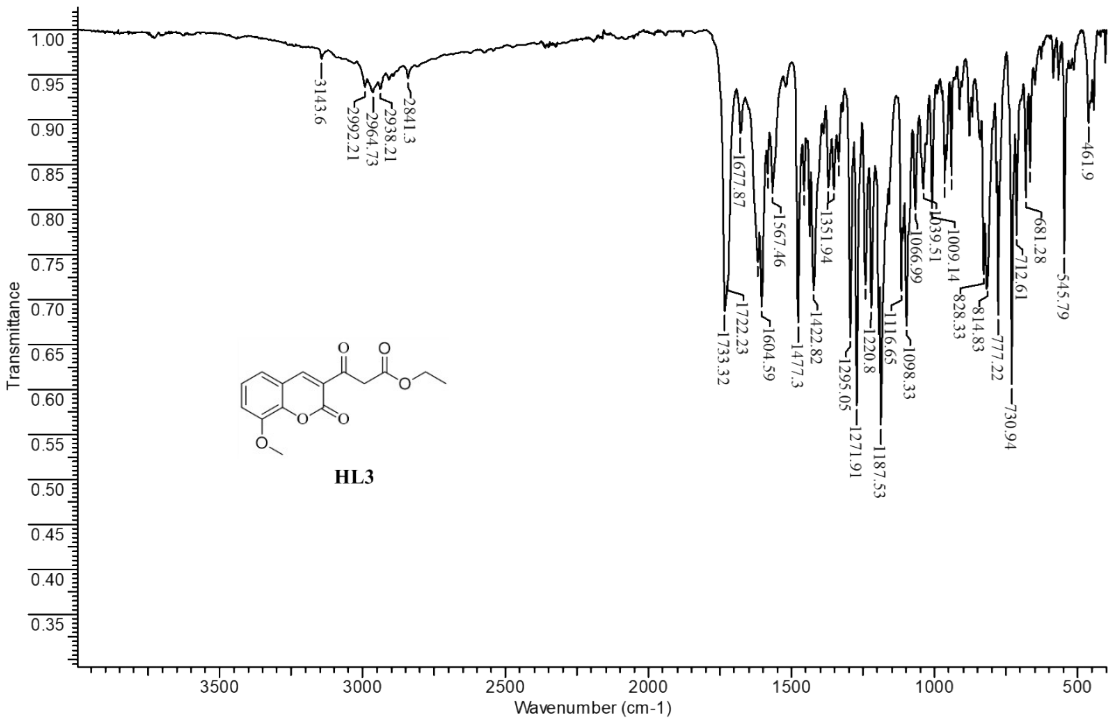

Figure S9: IR spectrum of **HL3**.

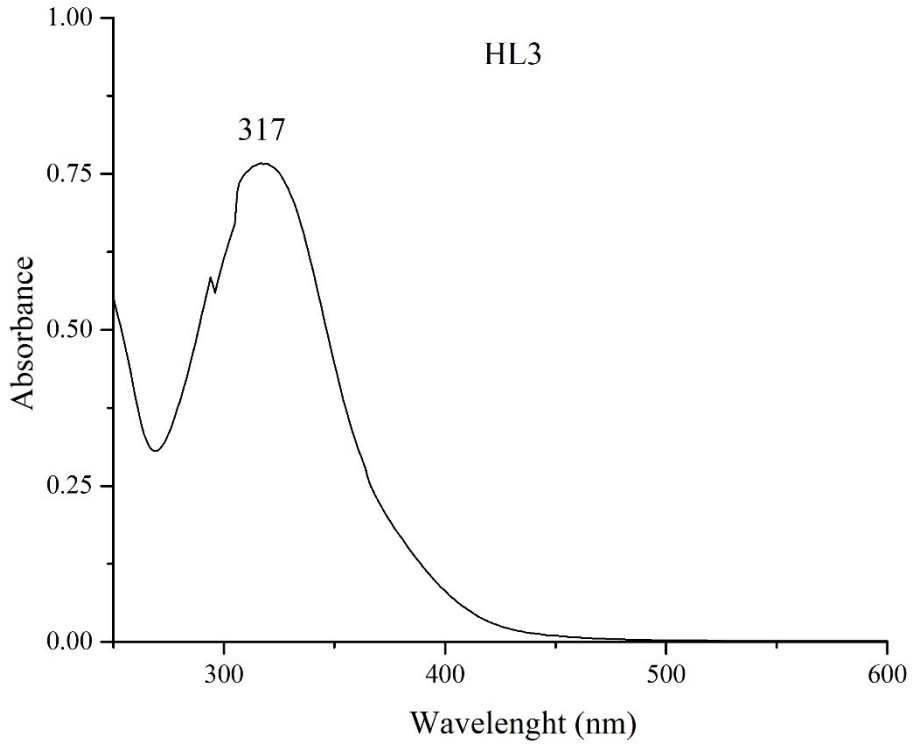

Figure S10: UV-Vis spectrum of **HL3** in phosphate buffer at 6 x 10^{-5} M.

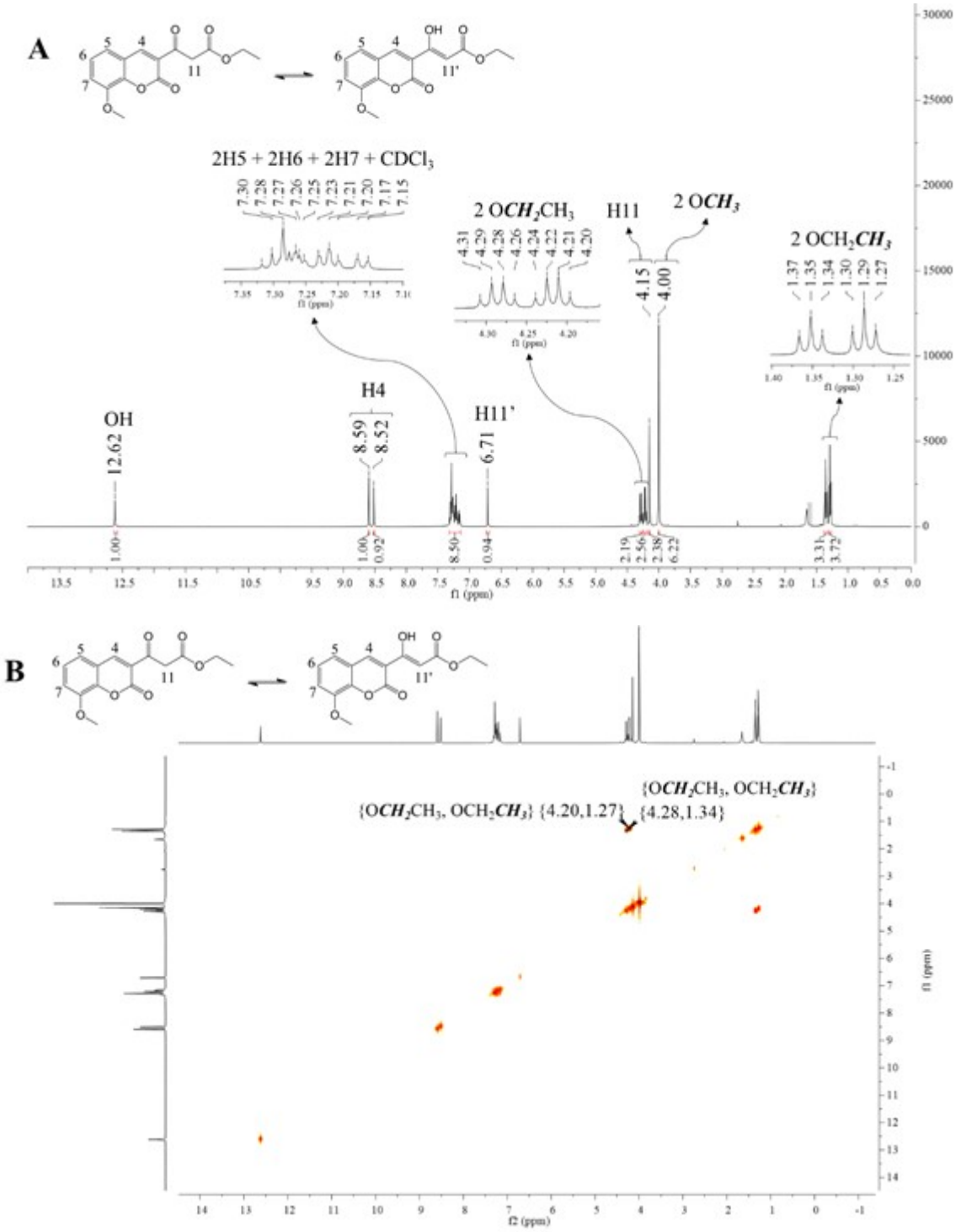

Figure S11: ^{1}H NMR spectrum of **HL3 (A)** and COSY spectrum **(B)**. Solvent: $CDCl_3$.

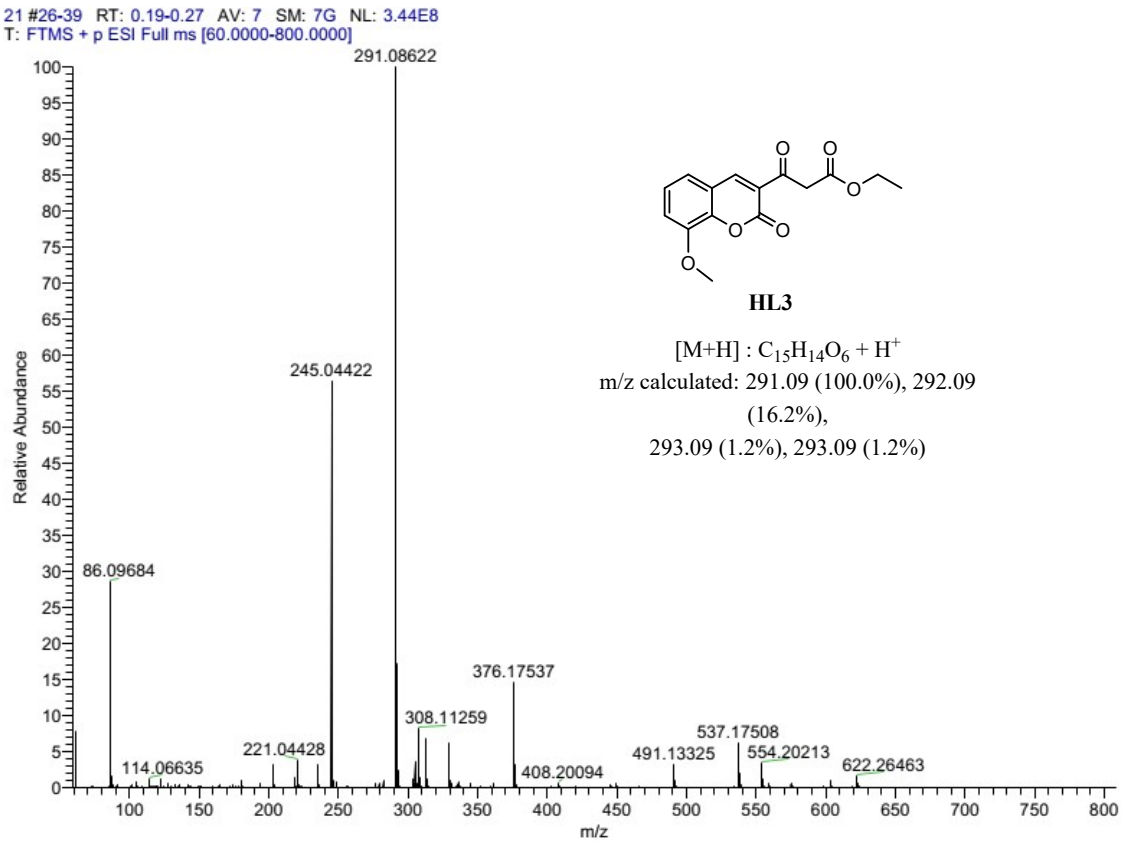

Figure S12: MS/ESI mass spectrum of **HL3**.

IV. *cis*-bis(2,2'-bipyridyl)-[3-(6-(methyl)-2-oxo-2*H*-chromen-3-yl)-3-oxoethylpropanoate]-ruthenium (II) hexafluorophosphate **(1)**

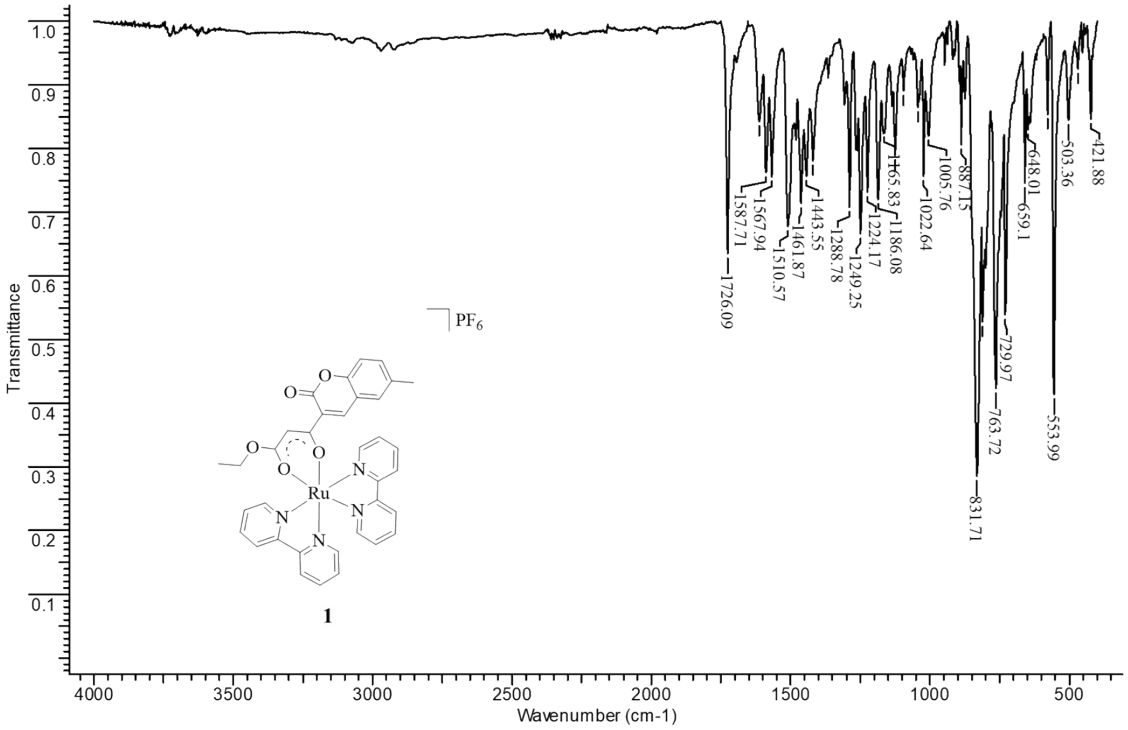

Figure S13: IR spectrum of **1**.

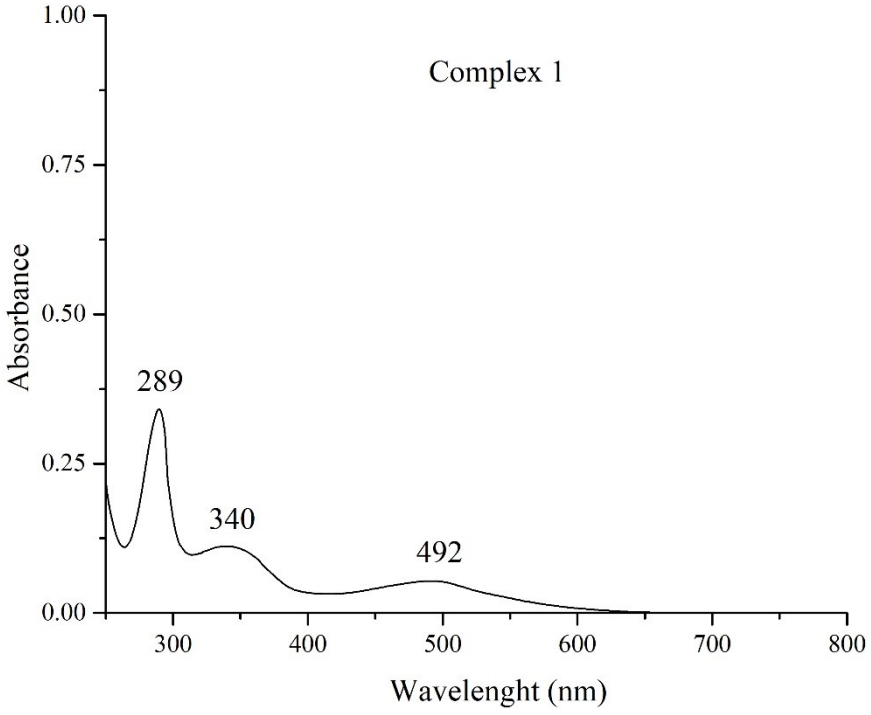

Figure S14: UV-Vis spectrum of **1** in phosphate buffer at 9 x 10^{-6} M.

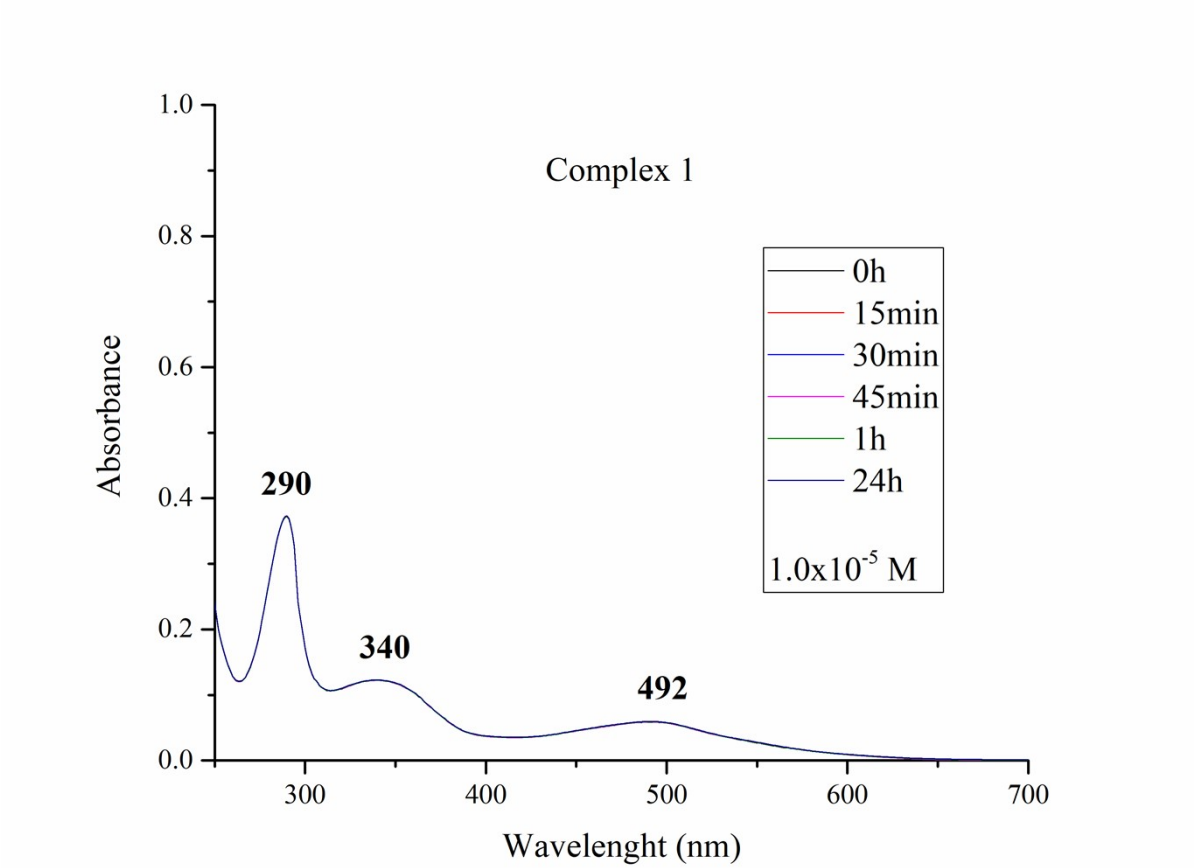

Figure S15: UV-Vis spectrum of **1** recorded over time within 24h, in phosphate buffer at 1.0 x 10^{-5} M.

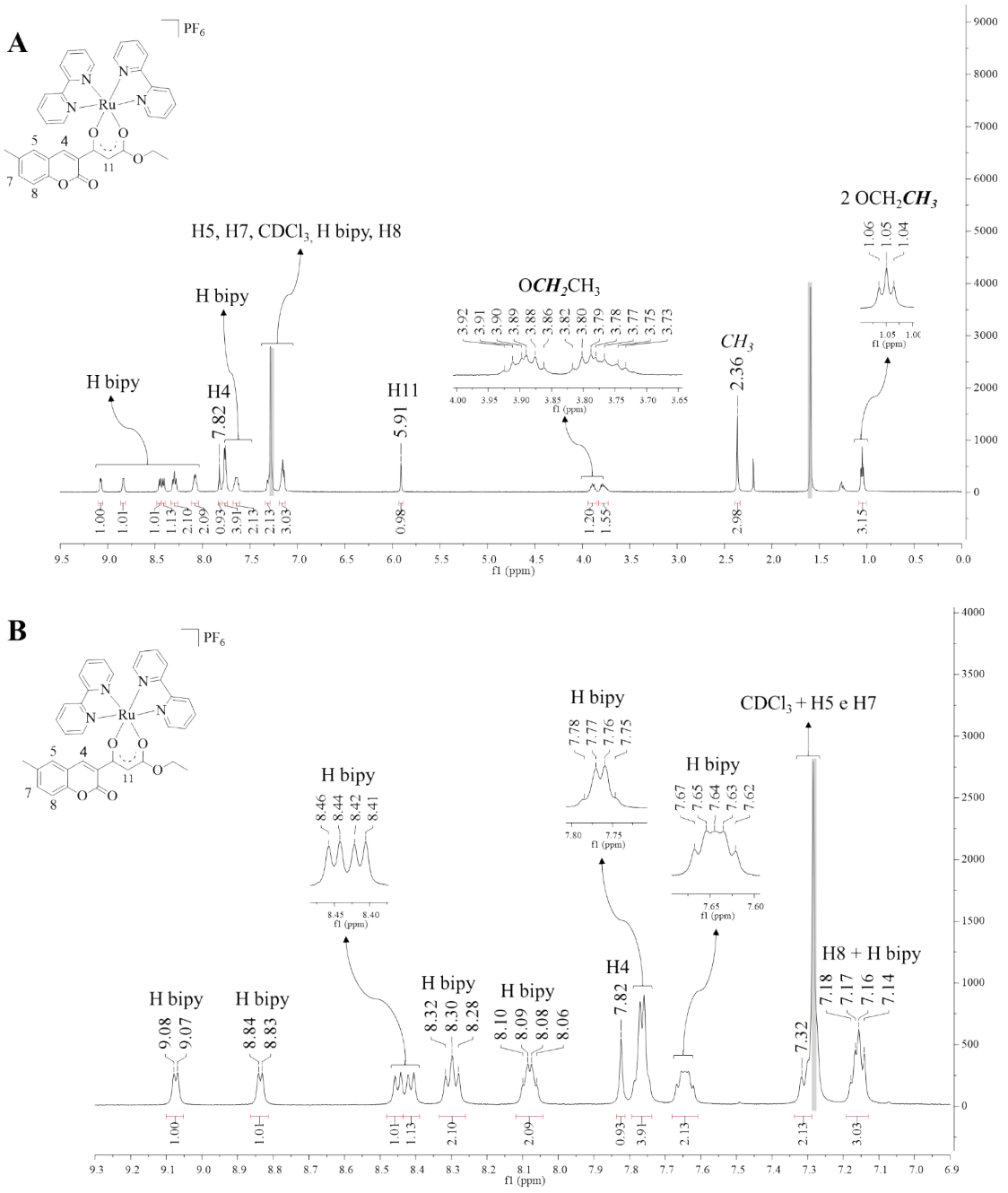

Figure S16: ^{1}H NMR spectra of **1** (**A**). Expanded region from 6.9 to 9.3 ppm (**B**). Solvent: $CDCl_3$.

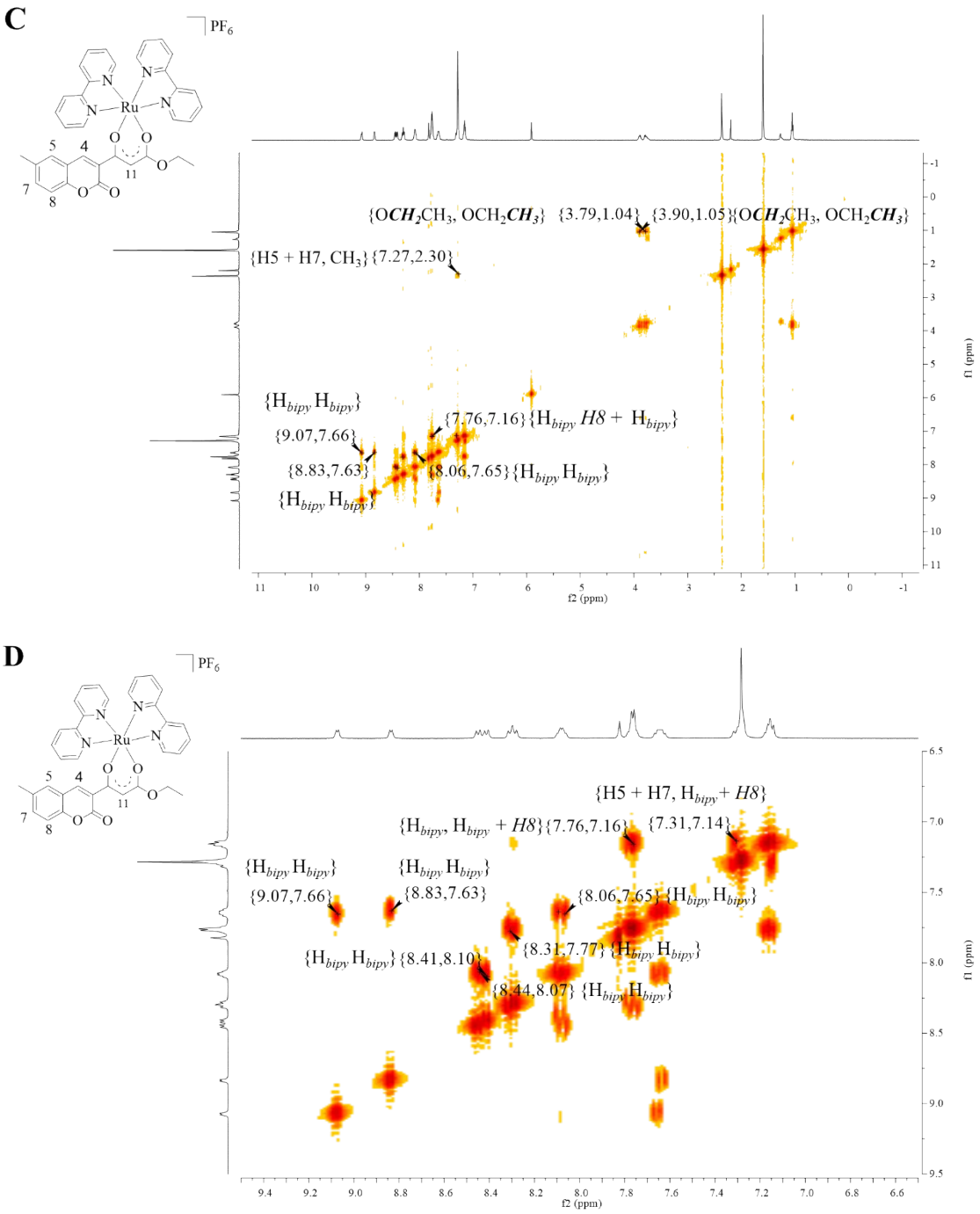

Figure S17: COSY spectra of **1** (**C**). Expanded region from 6.5 to 9.5 ppm (**D**). Solvent: $CDCl_3$.

V. *cis*-bis(2,2'-bipyridyl)-[3-(7-(diethylamino)-2-oxo-2*H*-chromen-3-yl)-3 oxoethylpropanoate] ruthenium (II) hexafluorophosphate **(2)**

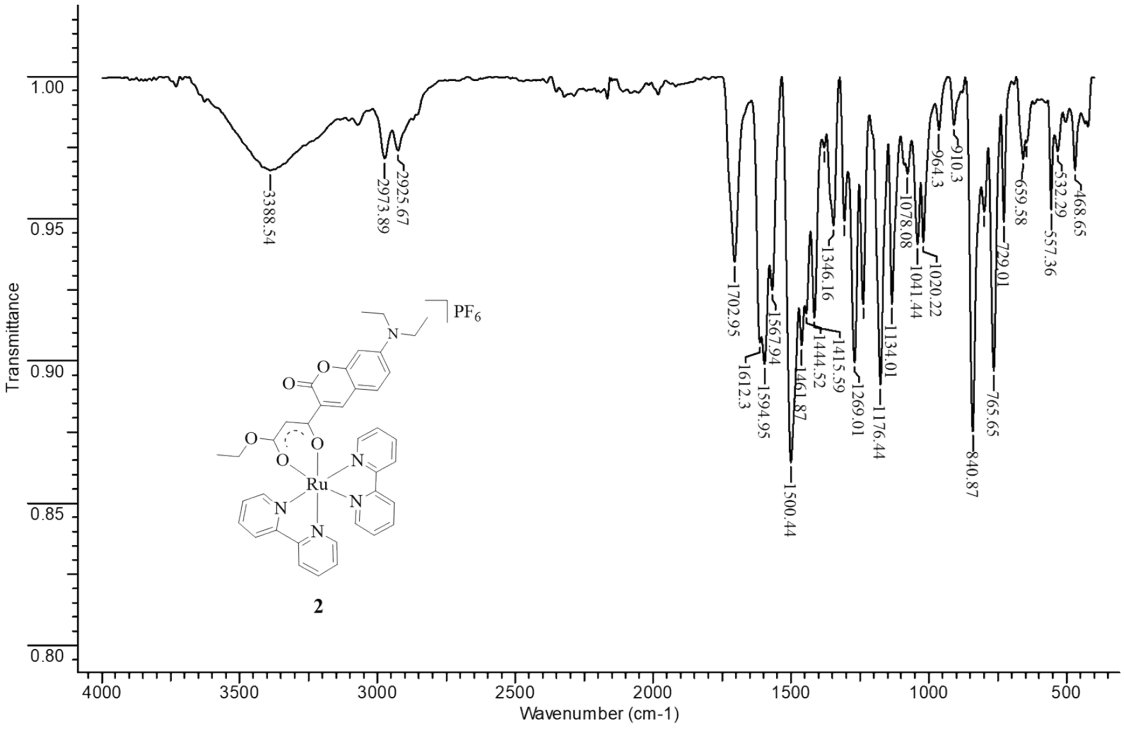

Figure S18: IR spectrum of **2**.

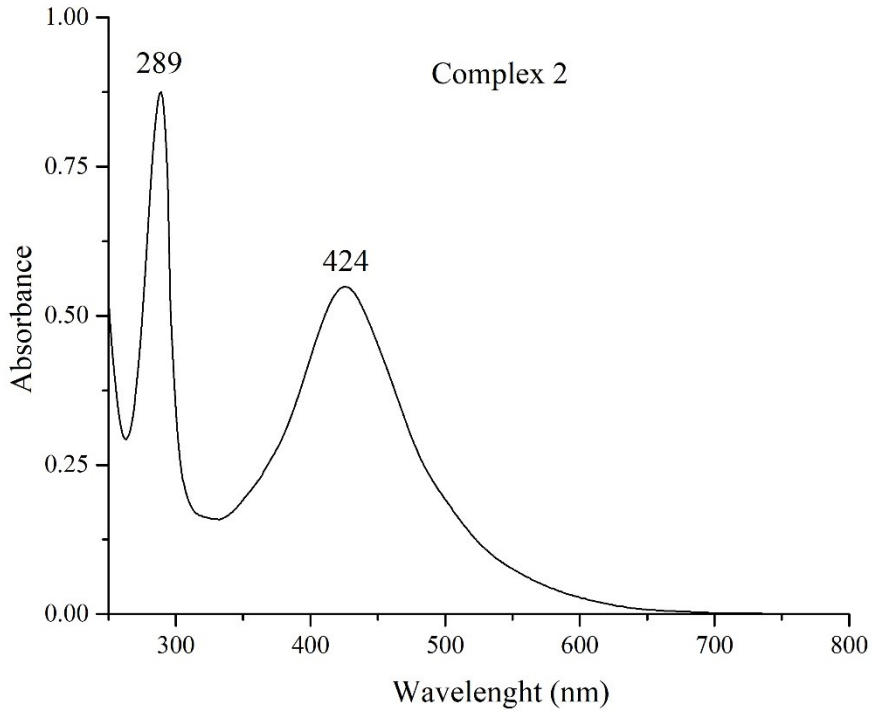

Figure S19: UV-Vis spectrum of the complex **2** in phosphate buffer at 2 x 10^{-5} M.

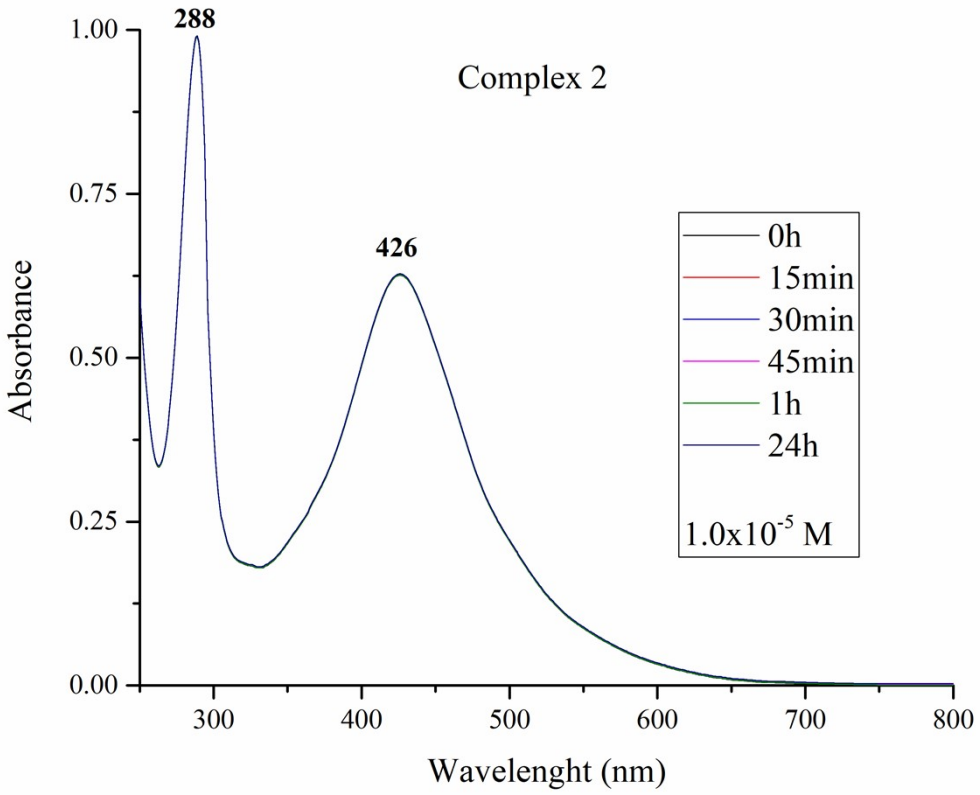

Figure S20: UV-Vis spectrum of **2** recorded over time within 24h, in phosphate buffer at 1.0 x 10^{-5} M.

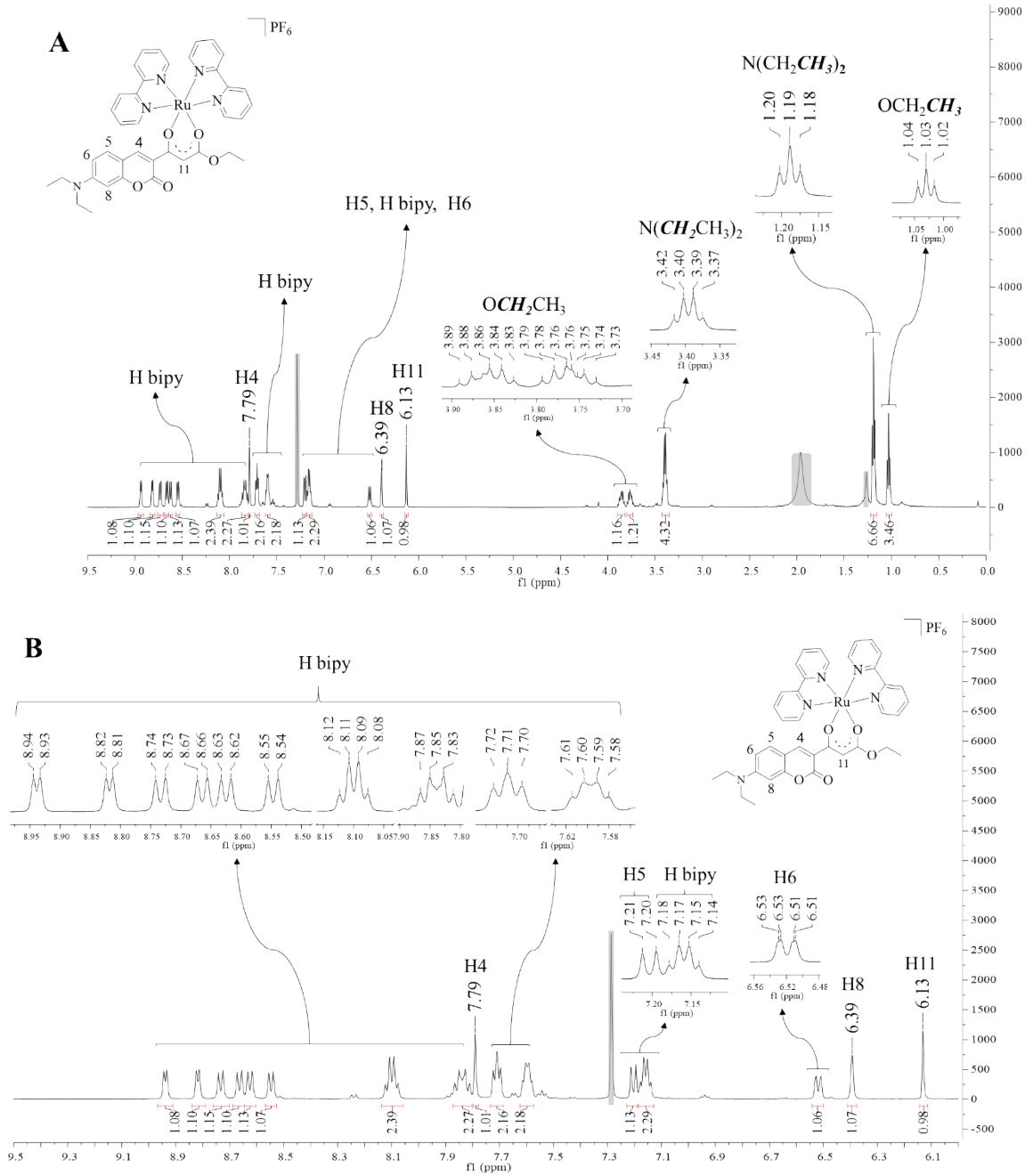

Figure S21: ^{1}H NMR spectra of **1** (**A**). Expanded region from 6.0 to 9.5 ppm (**B**). Solvent: $CDCl_3$

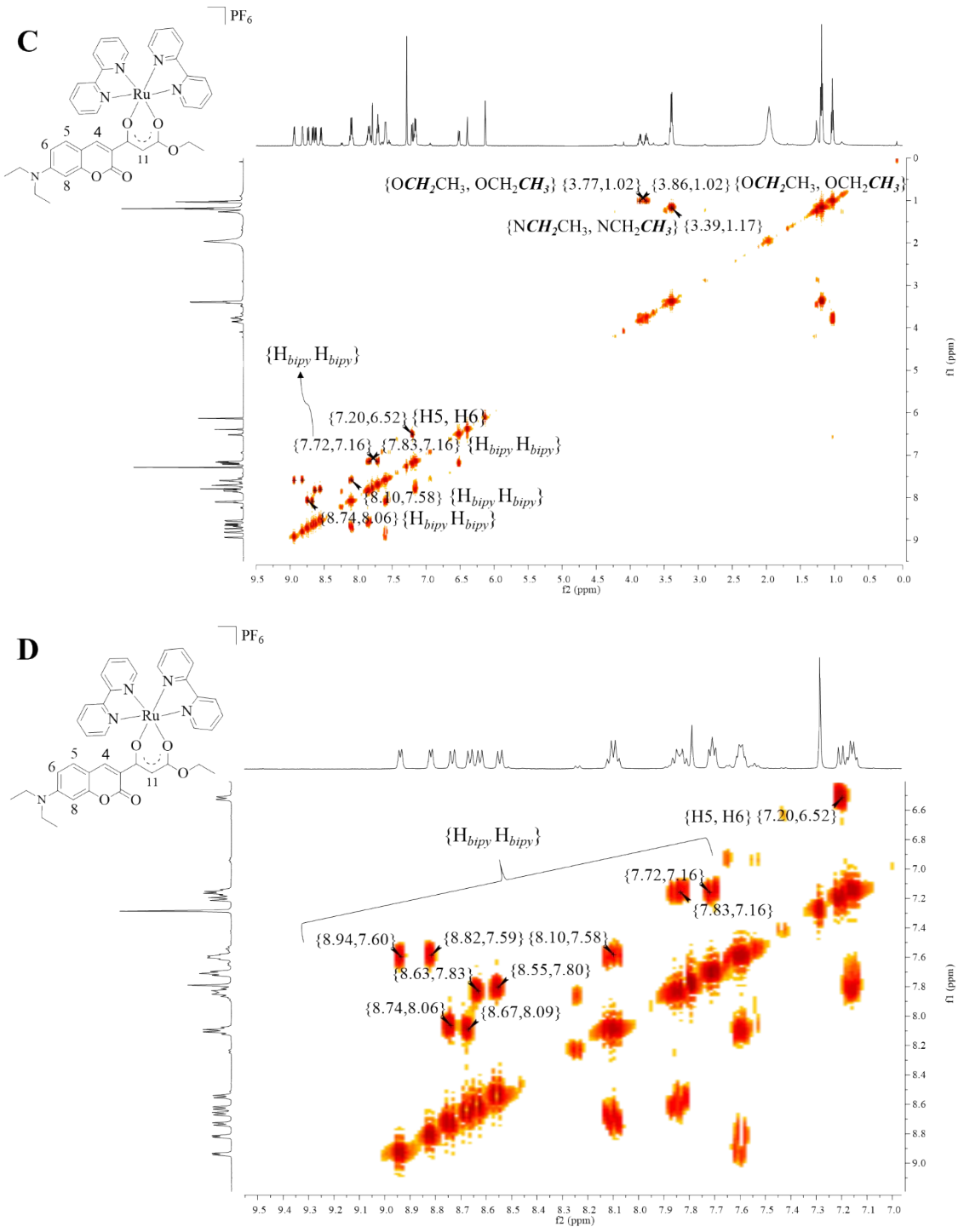

Figure S22: COSY spectra of **2** (**C**). Expanded region from 6.5 to 9.5 ppm (**D**). Solvent: $CDCl_3$.

VI. *cis*-bis(2,2'-bipyridyl)-[3-(8-(methoxy)-2-oxo-2*H*-chromen-3-yl)-3-oxoethylpropanoate] ruthenium (II) hexafluorophosphate **(3)**

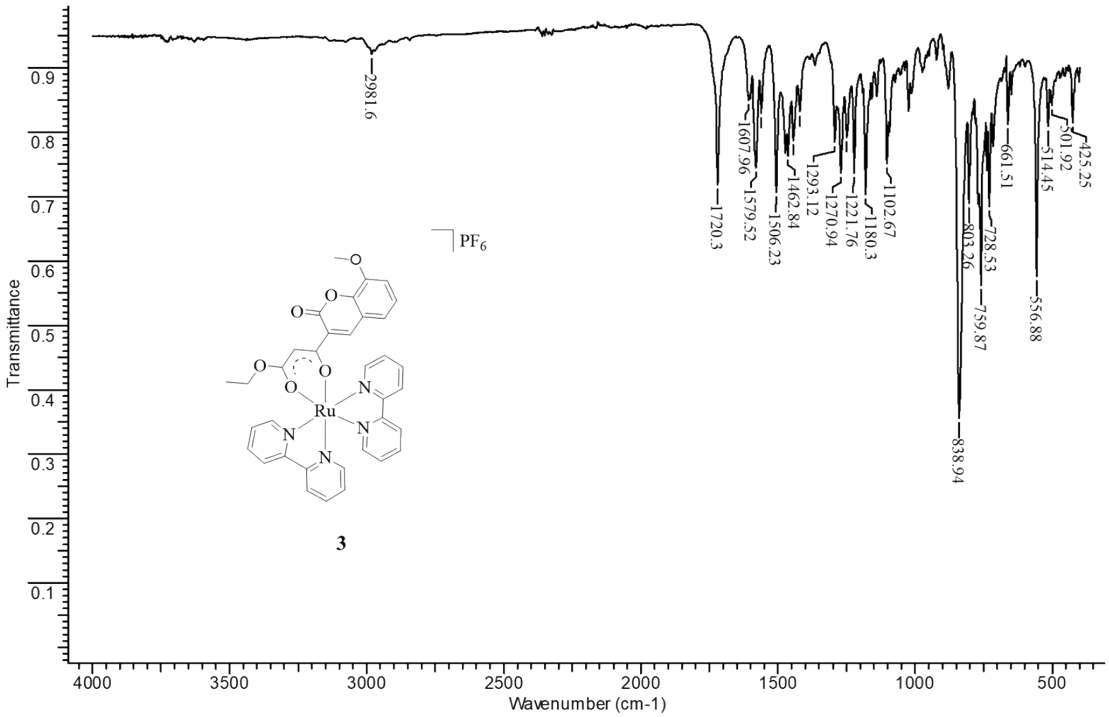

Figure S23: IR spectrum of **3**.

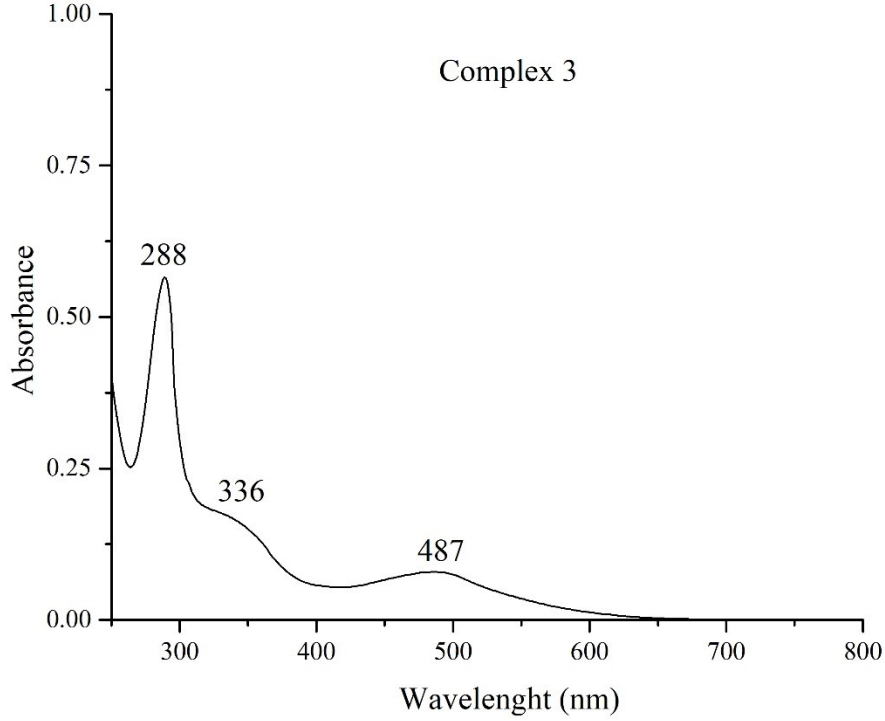

Figure S24: UV-Vis spectrum of **3** in phosphate buffer at 1.5 x 10^{-5} M.

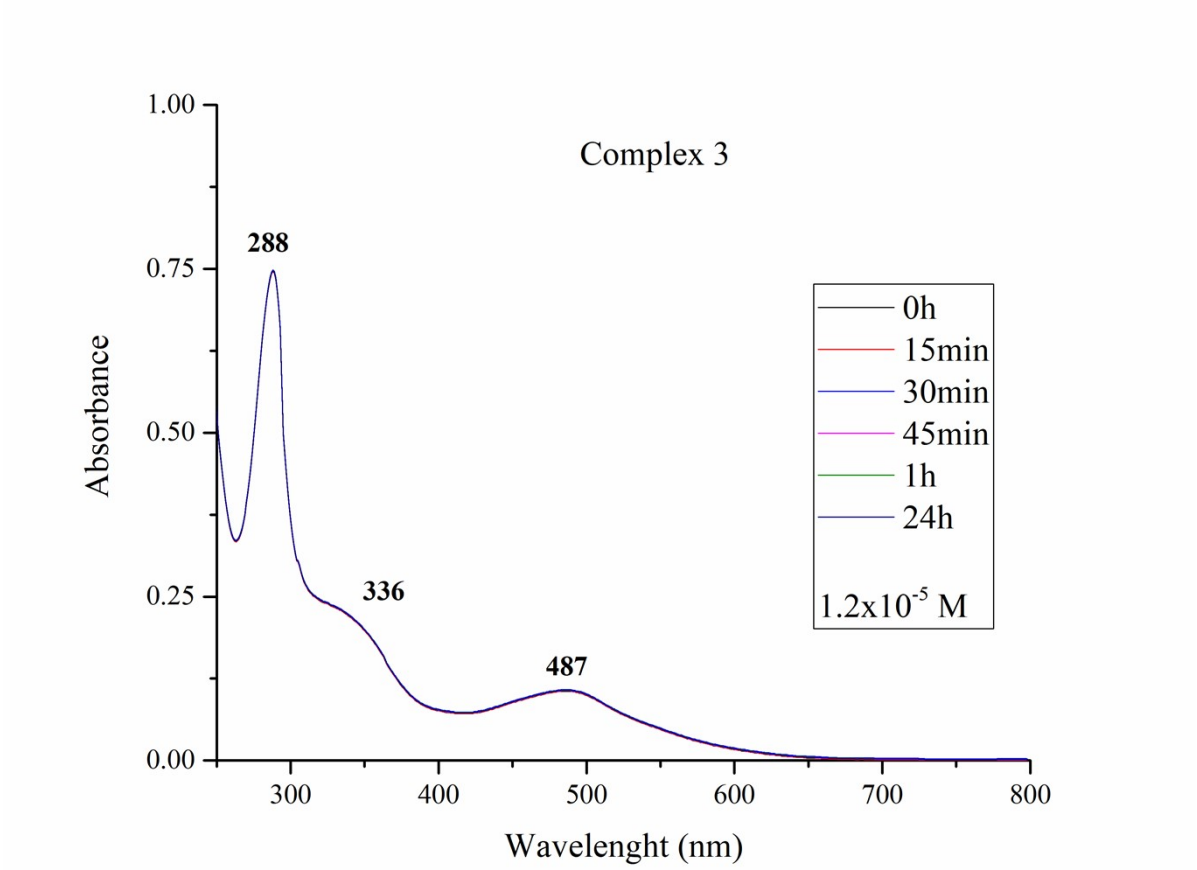

Figure S25: UV-Vis spectrum of **3** recorded over time within 24h, in phosphate buffer at 1.2 x 10^{-5} M.

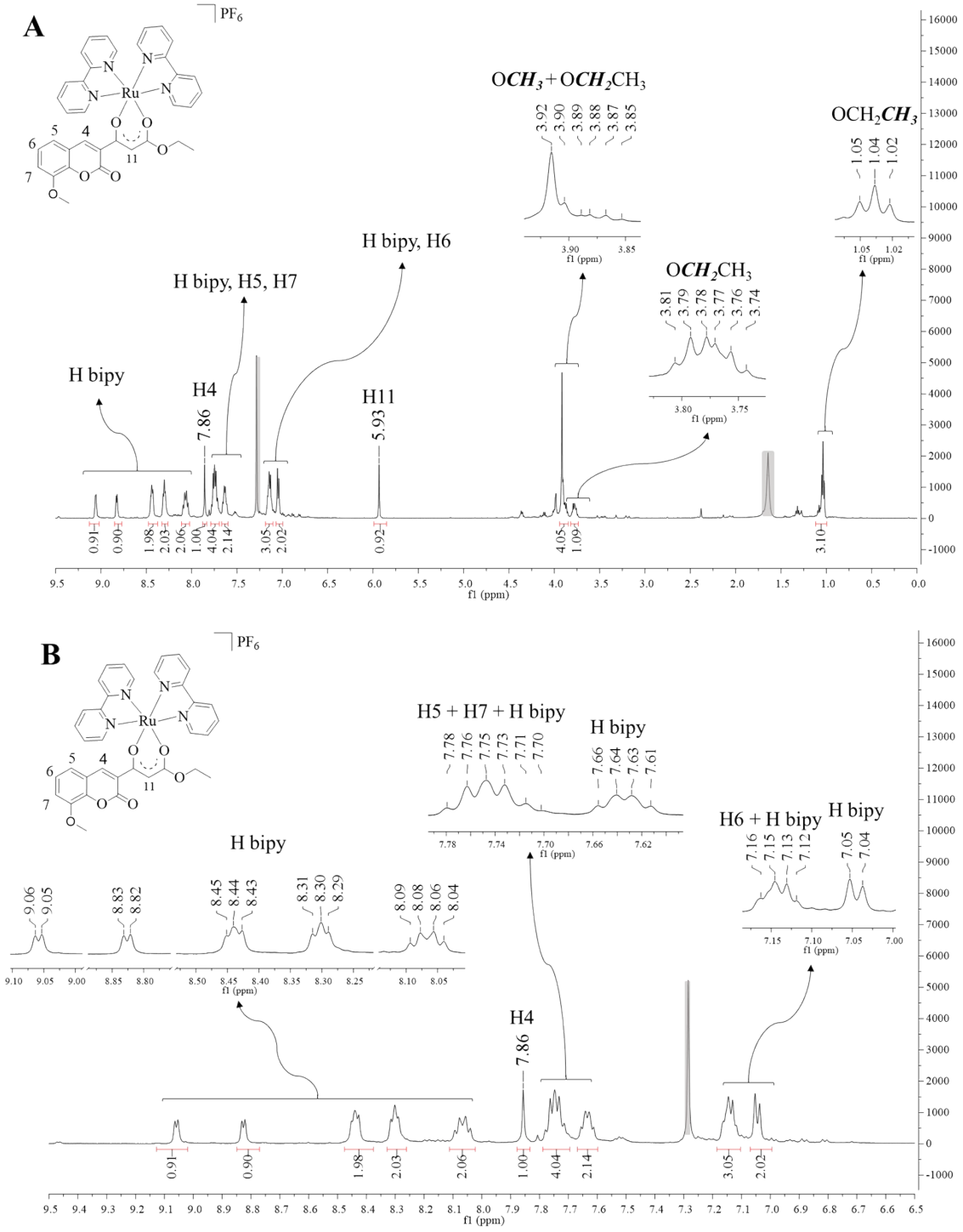

Figure S26: ^{1}H NMR spectra of **3** (**A**). Expanded region from 6.5 to 9.5 ppm (**B**). Solvent: $CDCl_3$

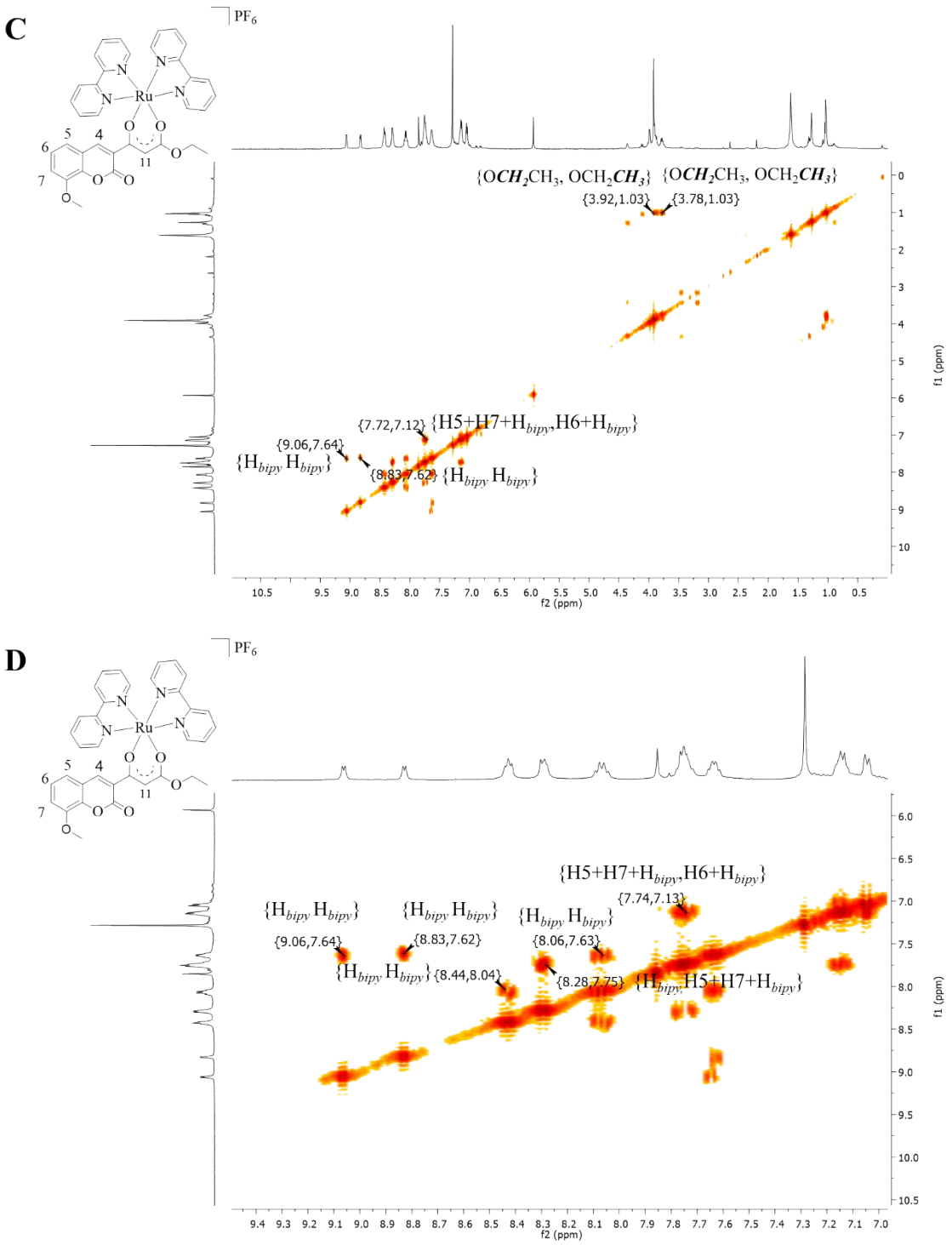

Figure S27: COSY spectra of **3** (**C**). Expanded region from 7.0 to 9.5 ppm (**D**). Solvent: CDCl3.

VII. X-Ray diffraction analysis

Table S1: Summary of crystal structure, data collection and refinement for complex **2**.

Chemical formula	$C_{38}H_{36}F_6N_5O_5PRu$
Formula weigh	888.76
Crystal system	monoclinic
a/Å	28.3360(12)
b/Å	10.5670(3)
c/Å	26.8770(9)
α/°	90
β/°	110.5490(10)
γ/°	90
Unit cell volume (Å^3)	7535.6(5)
T (K)	273(2)
Space group	C 2/c
Formula units per cell, *Z*	8
Radiation type	MoKα
Absorption coefficient (mm^{-1})	0.539
Reflections measured	41132
Independents reflections	6637
R_{int}	0.0521
Final R_1 values (I>2σ(I))	0.0361
Final $wR(F^2)$ values (I>2σ(I))	0.0773
Final R_1 values (all data)	0.0522
Final $wR(F^2)$ values (all data)	0.0849
Goodness of (GOF) fit F^2	1.046
CCDC deposition	2076893

Table S2: Hydrogen-bond geometry (Å, °) for **2.**

D—H···*A*	*D*—H	*H*···*A*	*D*···*A*	*D*—H···*A*
C35—H35...F5i	0.93	2.99	3.306(4)	101.4
C38—H38...O4	0.93	2.61	3.149(4)	117.8
C28—H28...F4	0.93	2.51	3.140(4)	125.5

Symmetry code: (i) -x+1, -y+2, -z+1.

VIII. Biological studies

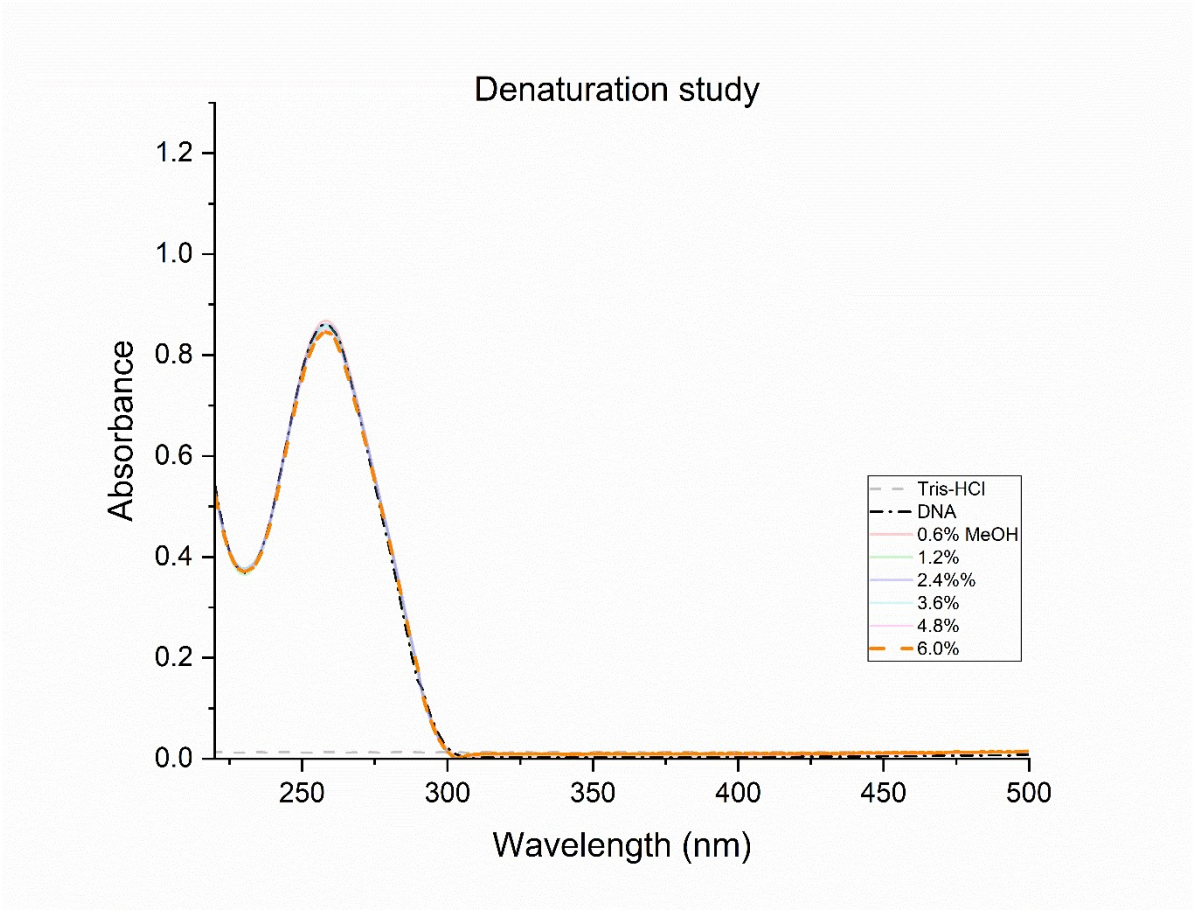

Figure S28. Absorption spectra of the ct-DNA in the presence of methanol in different proportions. Methanol = 0, 0.6, 1.2, 2.4, 3.6, 4.8 and 6.0%. ct-DNA at a concentration of 120 μ M in Tris-HCl buffer (pH 7.4).

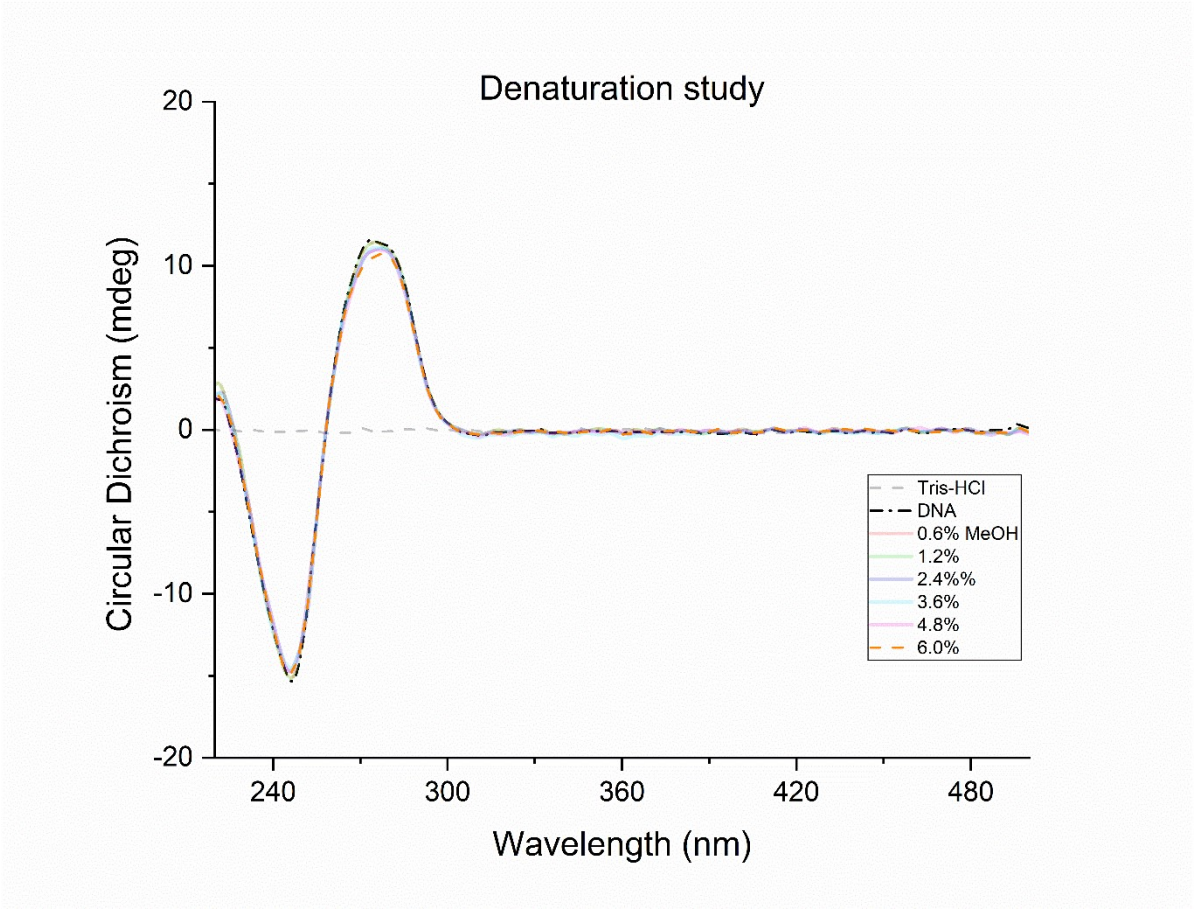

Figure S29. Circular dichroism of DNA at a concentration of 120 µM in Tris-HCl buffer (pH 7.4), in the presence of increasing methanol proportions (0 to 6 %).

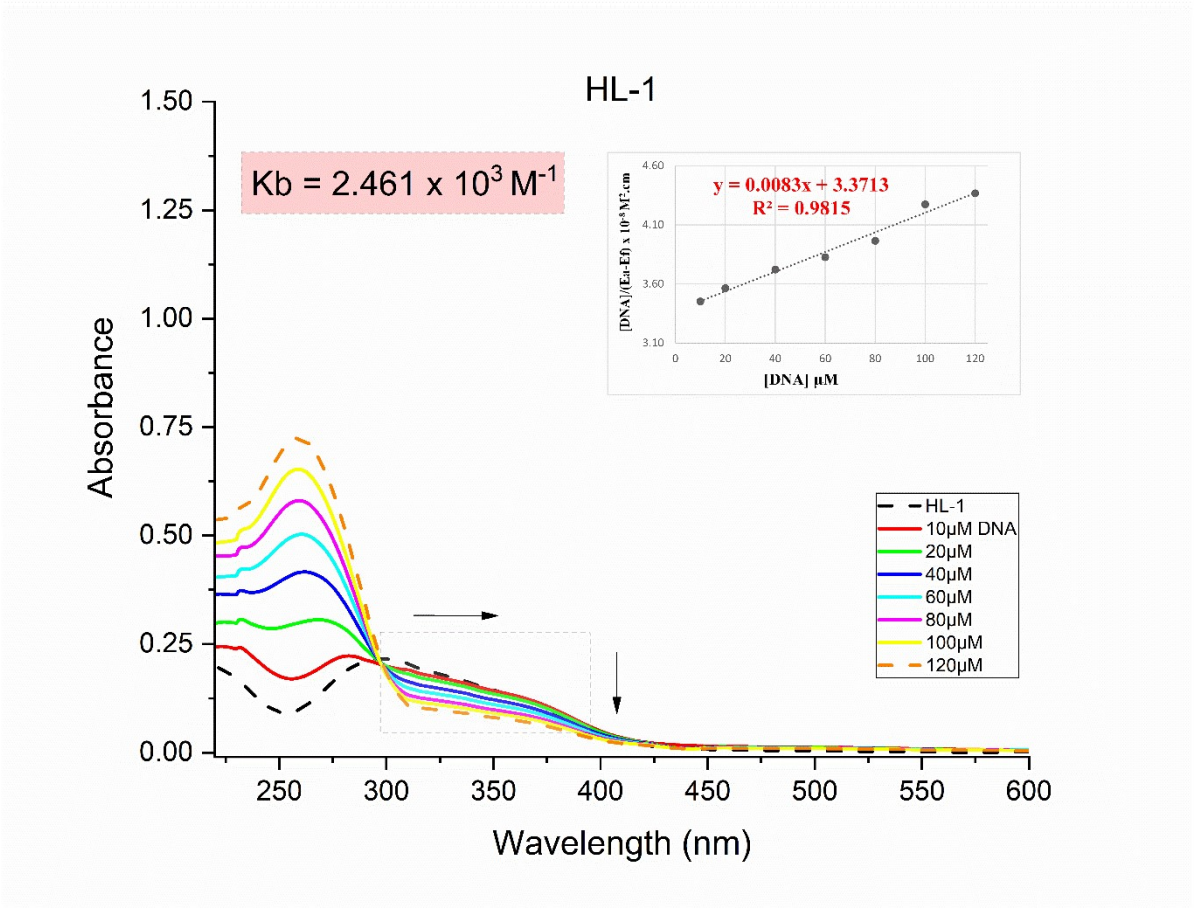

Figure S30. Absorption spectra of **HL1** at 30 µM in Tris-HCl buffer (pH 7.4) in the presence of ct-DNA in different concentrations. ct-DNA = 0, 10, 20, 40, 60, 80, 100 and 120 µM. λ (Kb) = 327 nm.

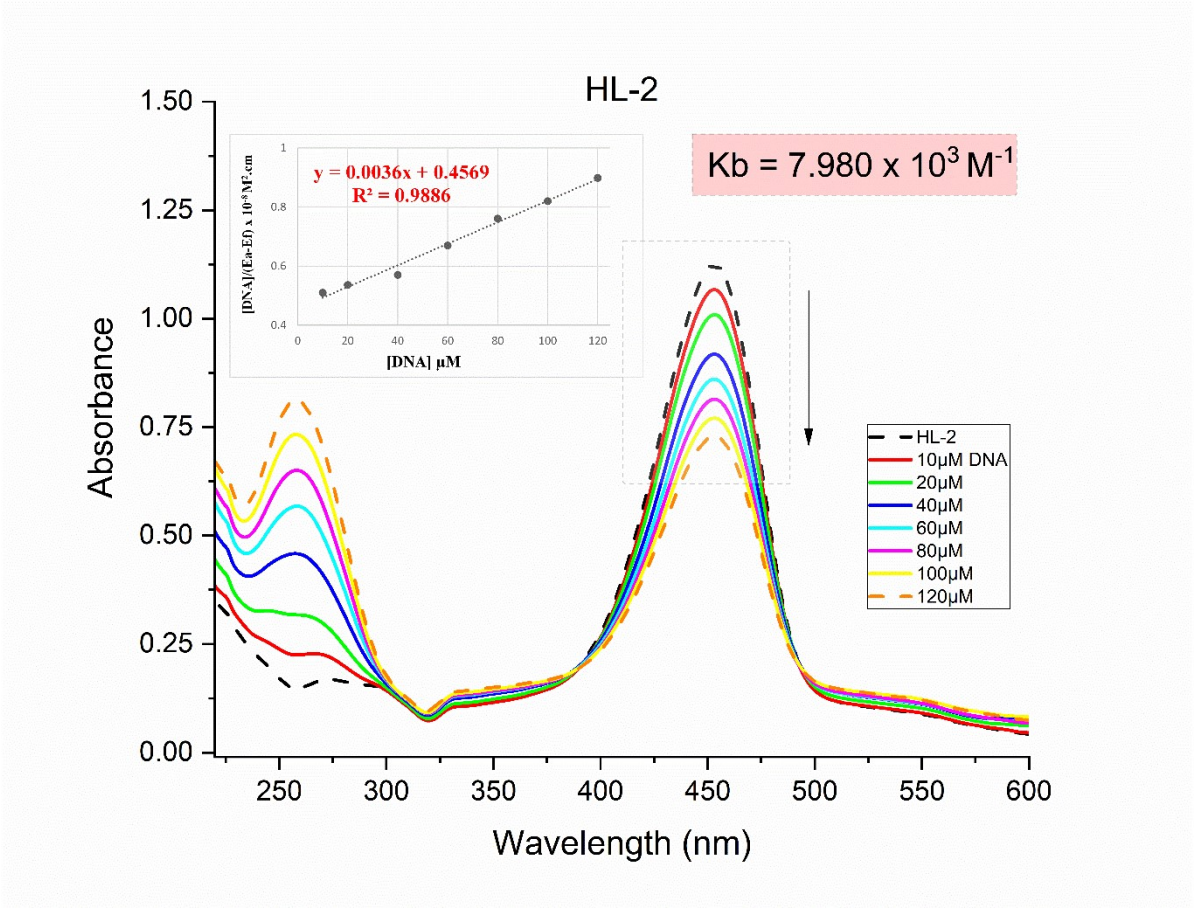

Figure S31. Absorption spectra of **HL2** at 30 µM in Tris-HCl buffer (pH 7.4) in the presence of ct-DNA in different concentrations. ct-DNA = 0, 10, 20, 40, 60, 80, 100 and 120 µM. λ (Kb) = 453 nm.

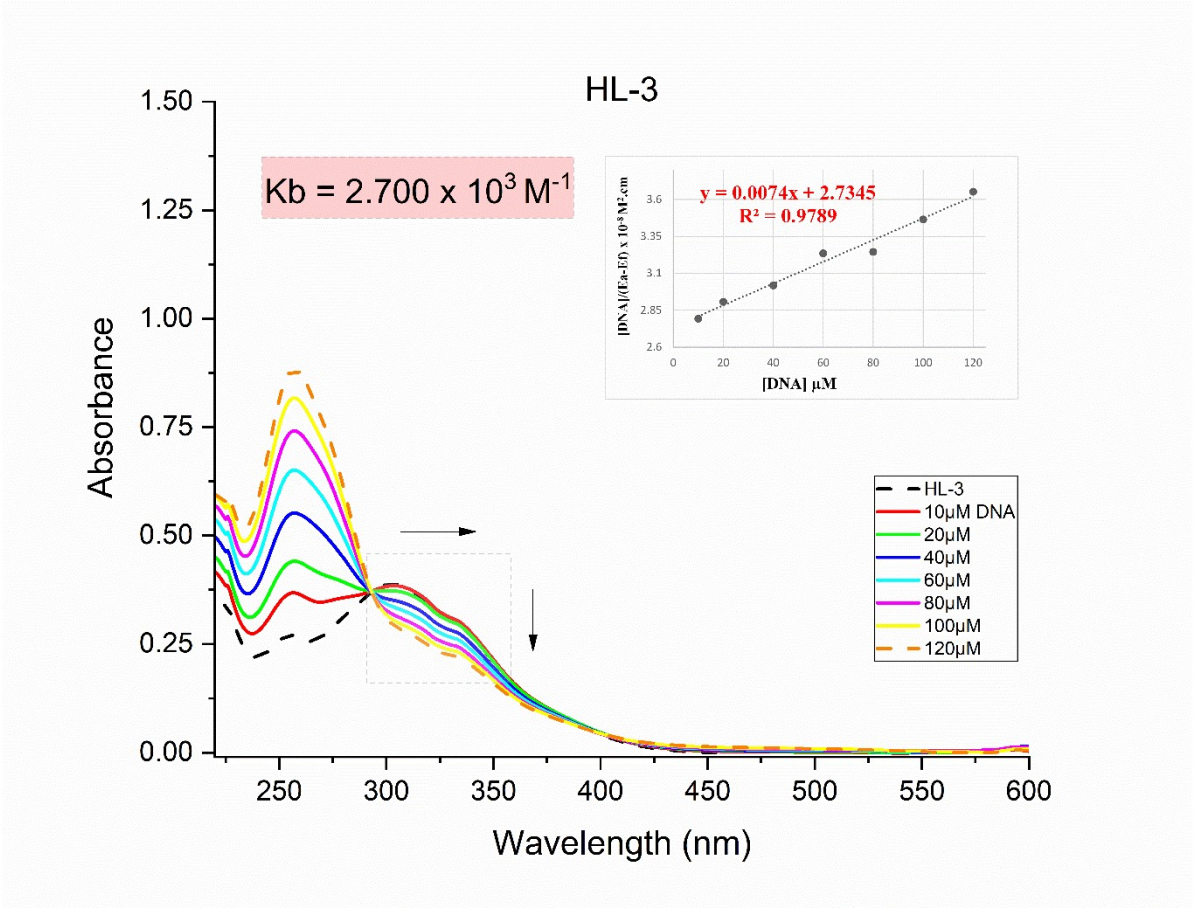

Figure S32. Absorption spectra of **HL3** at 30 µM in Tris-HCl buffer (pH 7.4) in the presence of ct-DNA in different concentrations. ct-DNA = 0, 10, 20, 40, 60, 80, 100 and 120 µM. λ (Kb) = 303 nm.

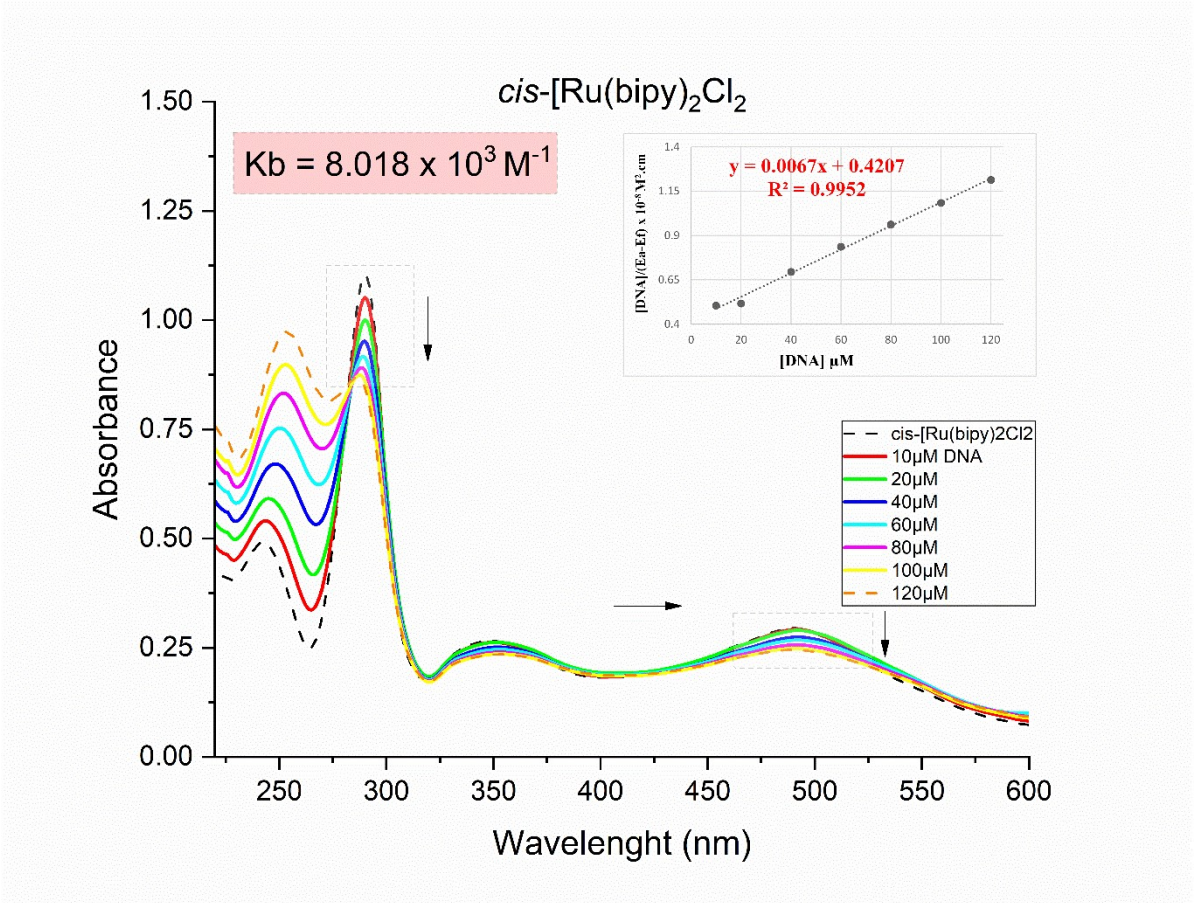

Figure S33. Absorption spectra of ***cis*-[Ru(bipy)$_2$Cl$_2$]** at 30 µM in Tris-HCl buffer (pH 7.4) in the presence of ct-DNA in different concentrations. ct-DNA = 0, 10, 20, 40, 60, 80, 100 and 120 µM. λ (Kb) = 490 nm.

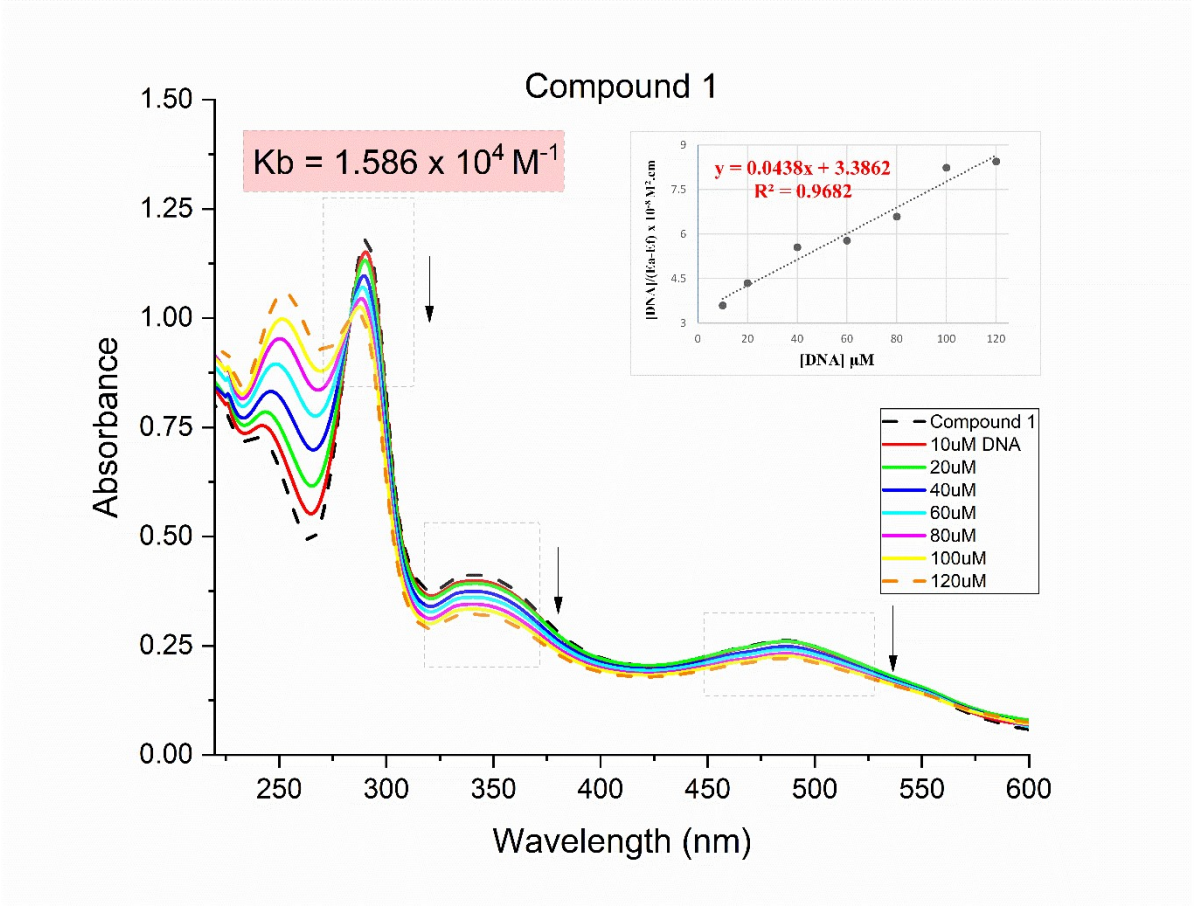

Figure S34. Absorption spectra of complex **1** at 30 µM in Tris-HCl buffer (pH 7.4) in the presence of ct-DNA in different concentrations. CtDNA = 0, 10, 20, 40, 60, 80, 100 and 120 µM. λ (Kb) = 487 nm.

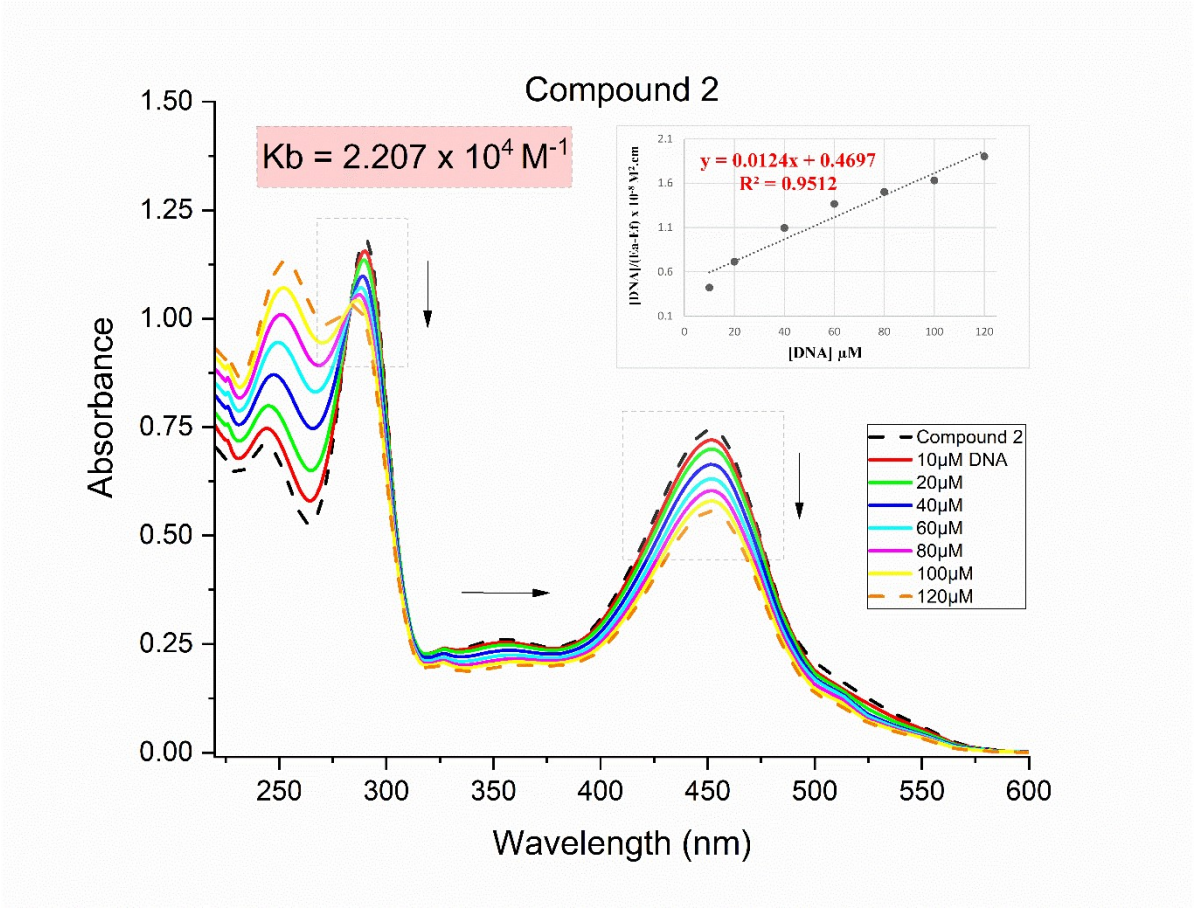

Figure S35. Absorption spectra of complex **2** at 30 µM in Tris-HCl buffer (pH 7.4) in the presence of ct-DNA in different concentrations. CtDNA = 0, 10, 20, 40, 60, 80, 100 and 120 µM. λ (Kb) = 450 nm.

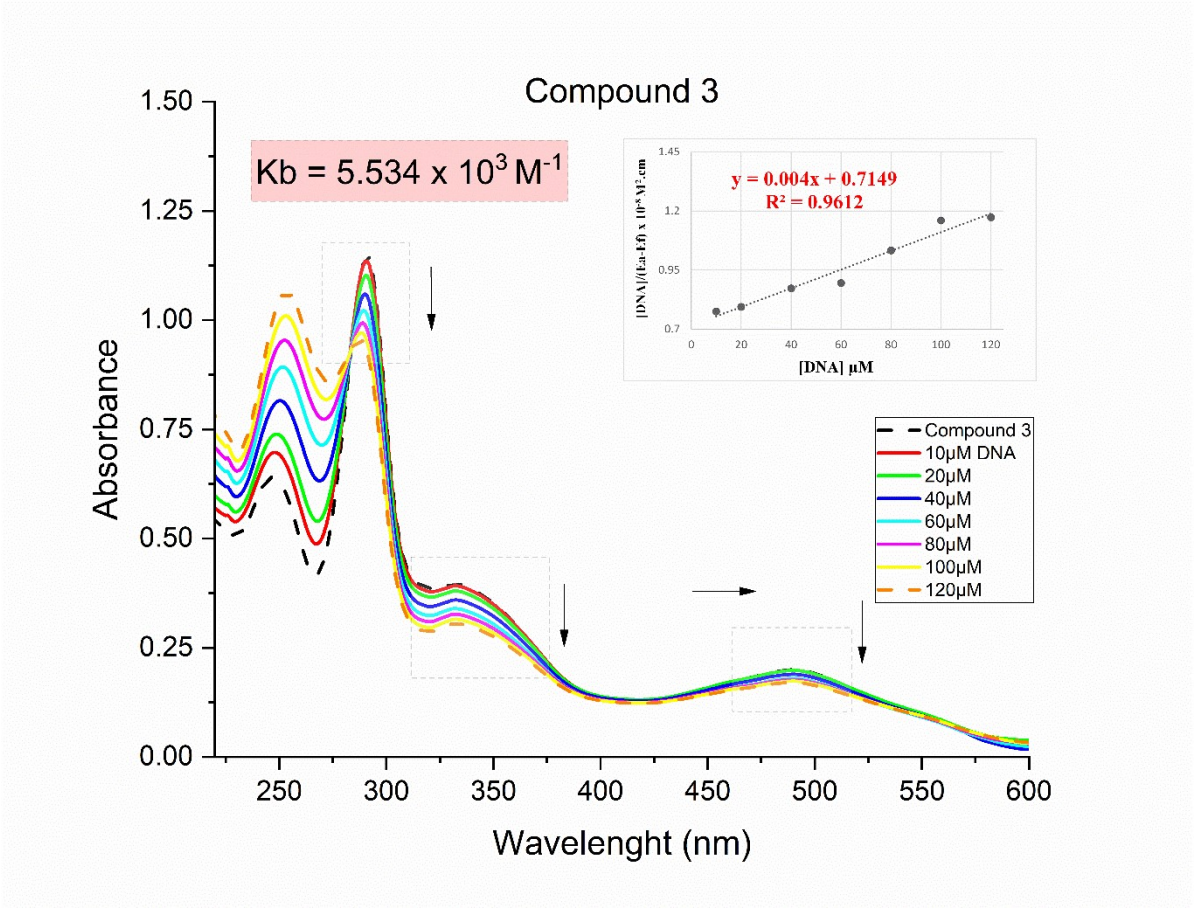

Figure S36. Absorption spectra of complex **3** at 30 µM in Tris-HCl buffer (pH 7.4) in the presence of ct-DNA in different concentrations. CtDNA = 0, 10, 20, 40, 60, 80, 100 and 120 µM. λ (Kb) = 490 nm.

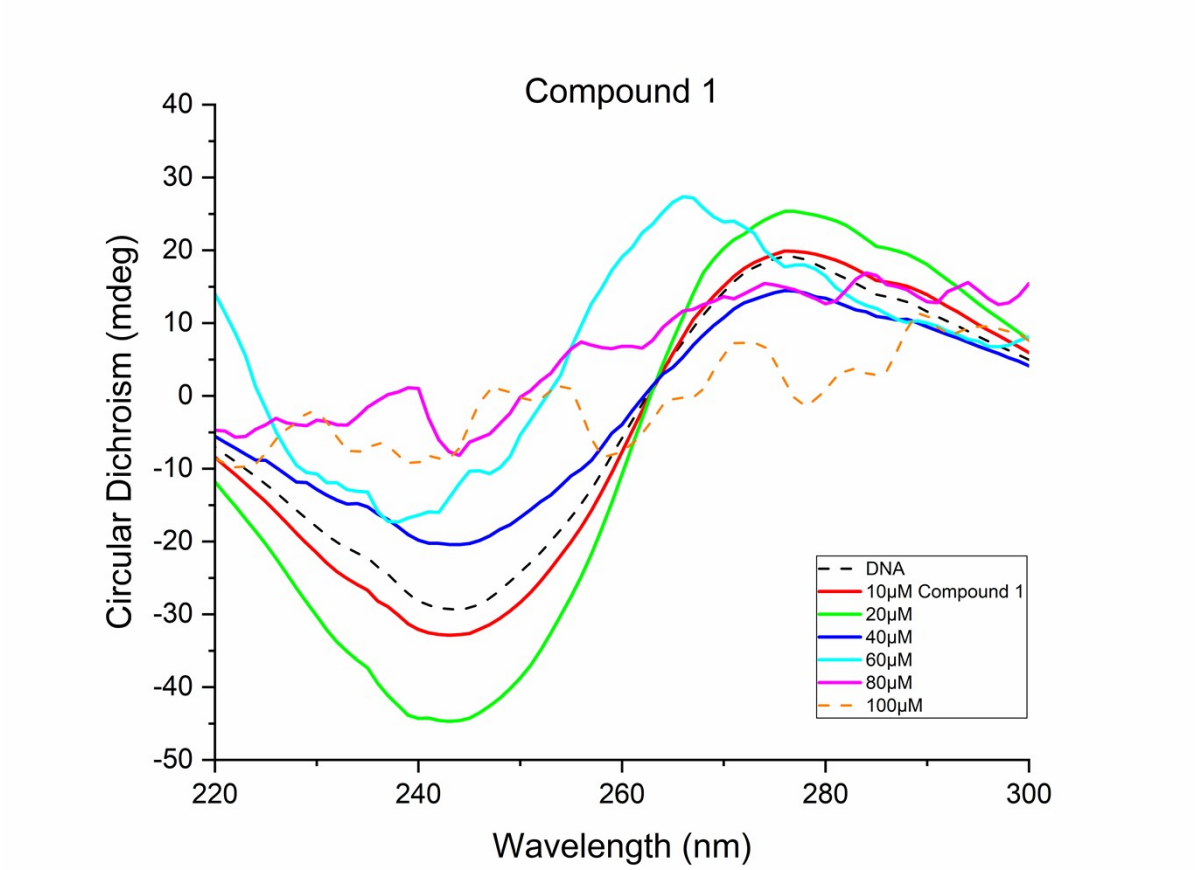

Figure S37. Circular dichroism of DNA at a concentration of 300 μM in Tris-HCl buffer (pH 7.4), in the presence of increasing concentrations of complex **1** (10, 20, 40, 60, 80 and 100 μM).

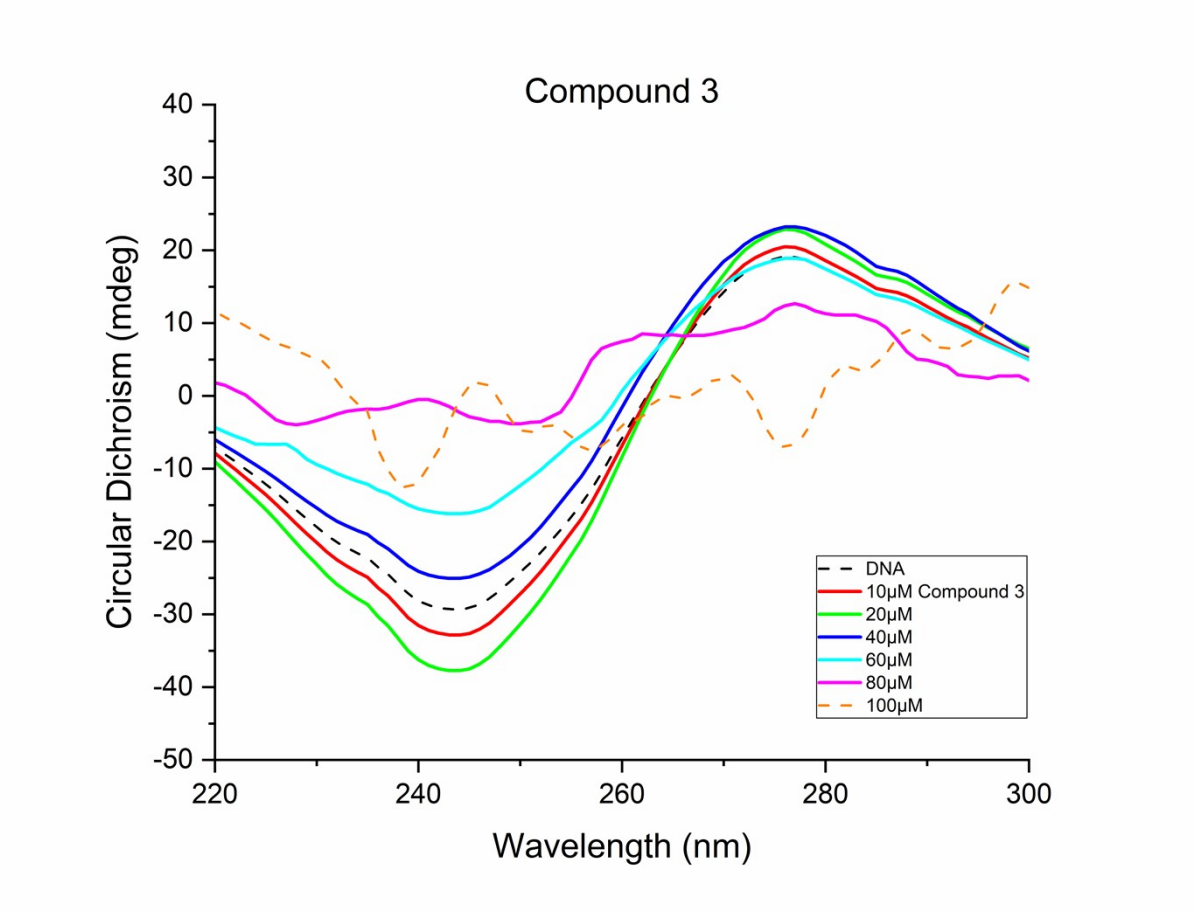

Figure S38. Circular dichroism of DNA at a concentration of 300 μM in Tris-HCl buffer (pH 7.4), in the presence of increasing concentrations of complex **3** (10, 20, 40, 60, 80 and 100 μM).

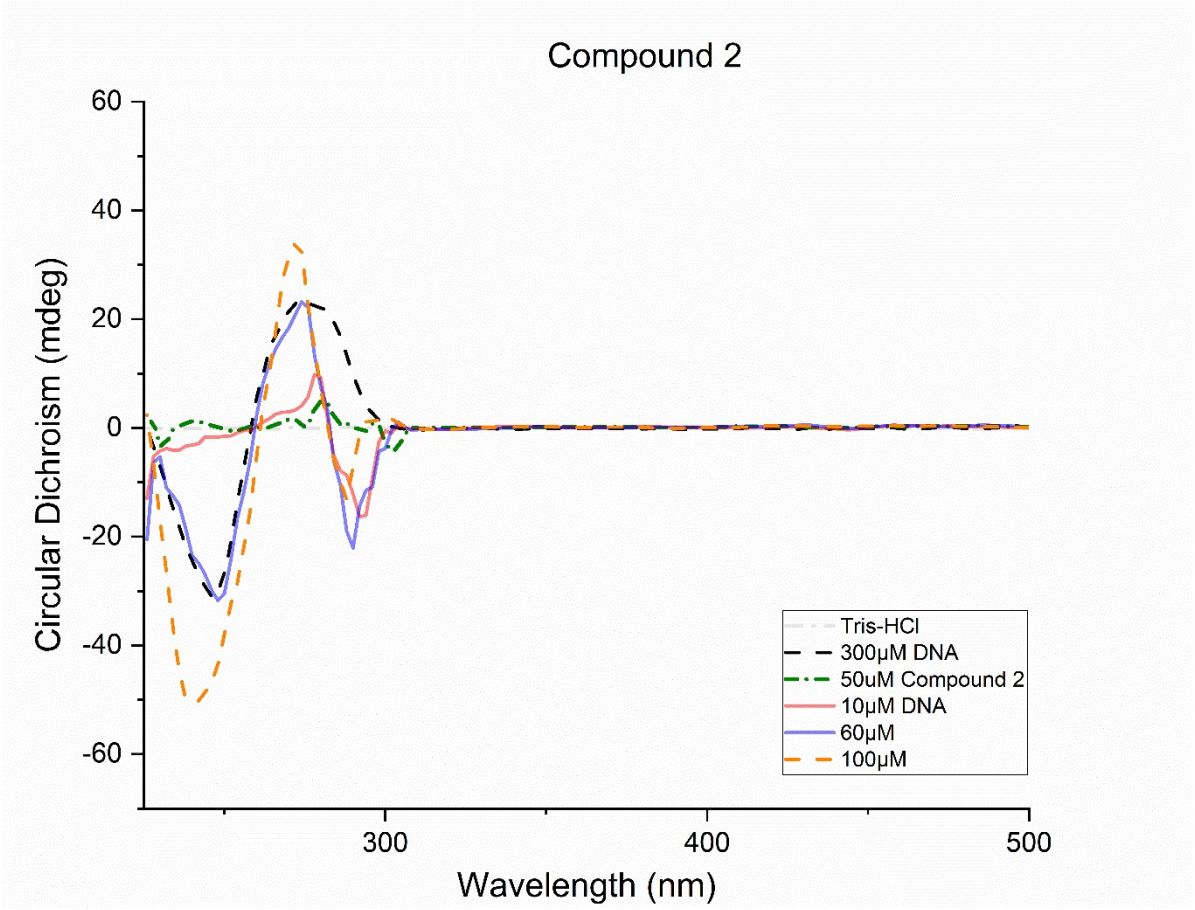

Figure S39. Circular dichroism spectra of the ct-DNA at different concentrations ([DNA] = 10, 60 and 100 μM) in the presence of compound **2** at 50 μM in Tris-HCl buffer (pH 7.4).

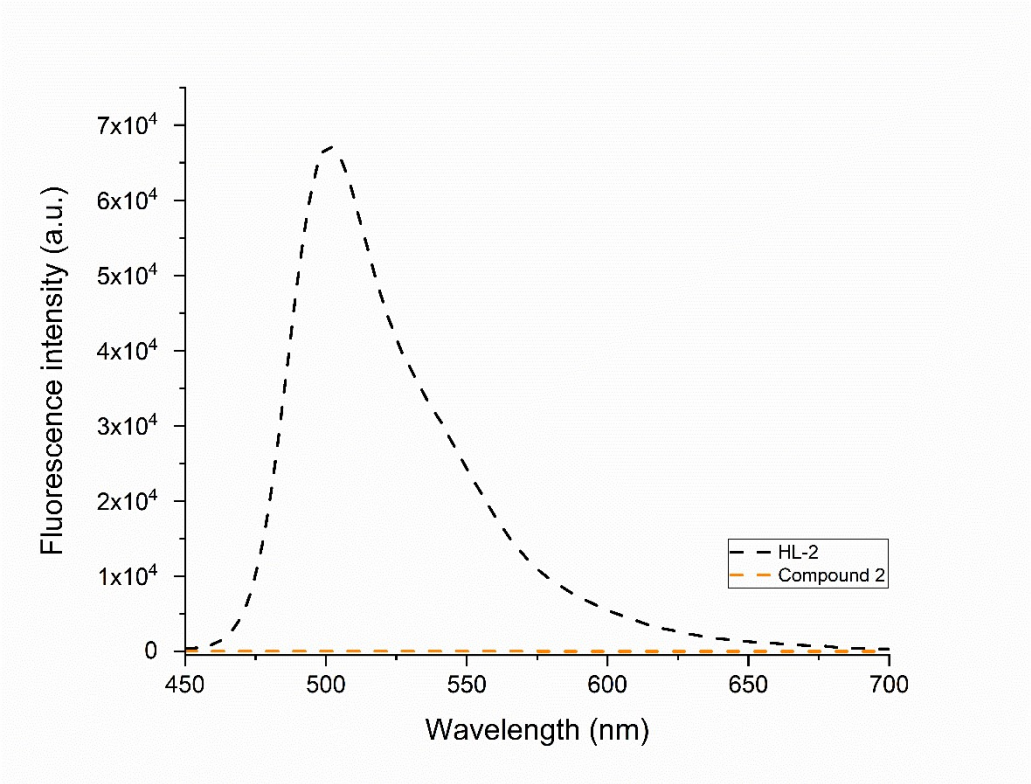

Figure S40. Fluorescence emission spectra of **HL2** and **2**, obtained at 50 μM (λex = 440 nm) in Tris-HCl buffer (pH 7.4) and recorded in an Edinburgh FLS980 spectrofluorometer.

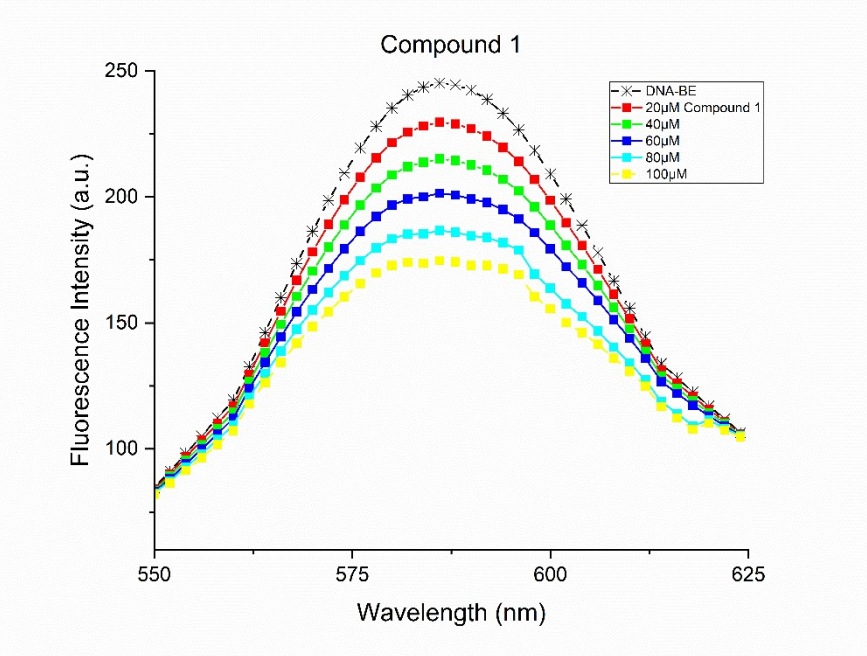

Figure S41. Emission quenching curves of EtdBr-DNA by complex **1** ([EtBr] = 10 μM, [DNA] = 100 μM, [Complex] = 0–100 μM.

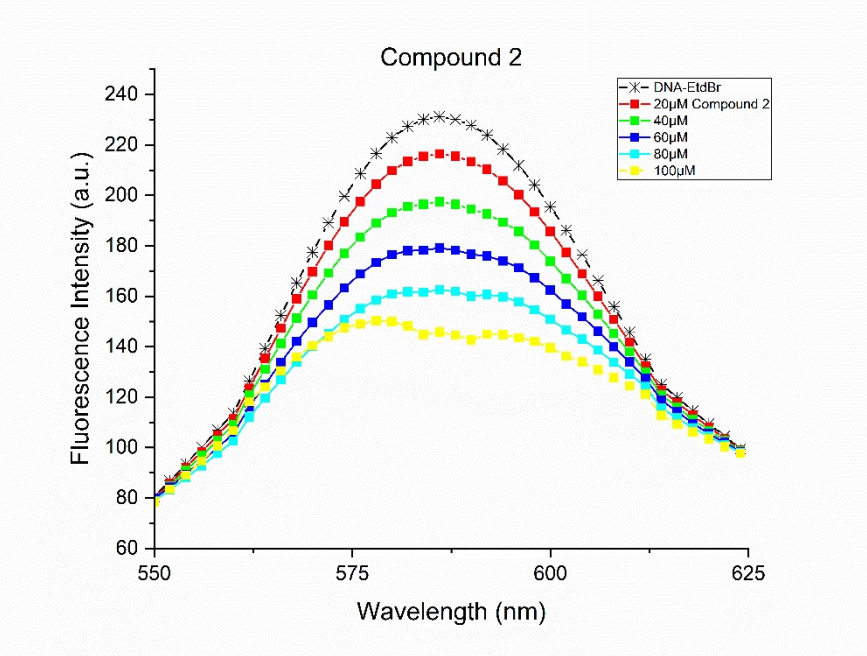

Figure S42. Emission quenching curves of EtdBr-DNA by complex **2** ([EtBr] = 10 μM, [DNA] = 100 μM, [Complex] = 0–100 μM.

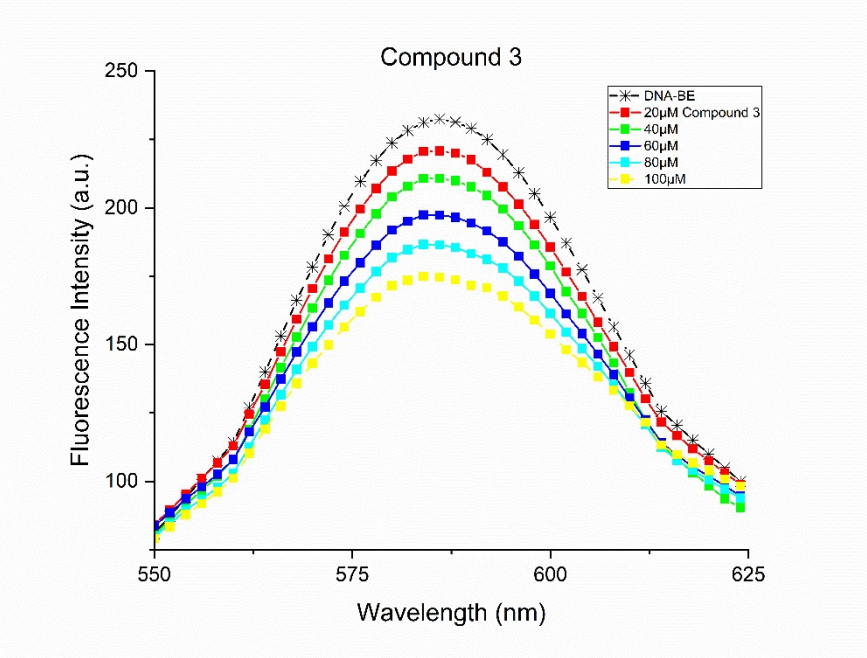

Figure S43. Emission quenching curves of EtdBr-DNA by complex **3** ([EtBr] = 10 μM, [DNA] = 100 μM, [Complex] = 0–100 μM.

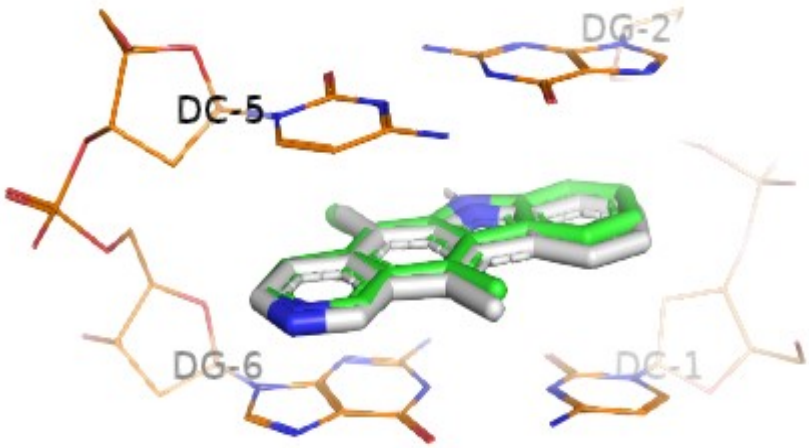

Figure S44. Redocking for target 1Z3F, available in PDB, Structure of ellipticine in complex with a 6-bp DNA, RMSD = 0.45.

Table S3: Molecular docking results for 1Z3F (PDB)**.**

COMPOUNDS	SCORE
1	67.28
2	68.62
3	64.88
Ellipticine	75.45 (RMSD 0.45)